2026

INTERNSHIP REPORT

Refining the Structural Maps of the Onshore Salt Diapir and the Offshore Salt Diapir

Research Report

Sep 2025 – Feb 2026

Internship Report for COVRA N.V. by:
Daxi Zheng

Supervised by:

Jeroen Bartol (COVRA N.V.)

Liviu Matenco (Utrecht University)

COVRA N.V.

Universiteit Utrecht

Abstract

Radioactive waste is currently stored in surface facilities at the Central Organization for Radioactive Waste (COVRA) in Zeeland. However, this storage is temporary, and the Netherlands is currently evaluating geological disposal in a stable environment, with a final selection of a disposal method and site planned for around 2050. Domal salt is under consideration as a host rock because its near-zero permeability and creep behaviour allow it to seal fractures and isolate waste from the biosphere. This necessitates a better understanding of the geological stability and mechanical integrity of Zechstein salt structures to consider effective long-term management of high-level radioactive waste in the Netherlands.

This study refines 3D structural models of the Pieterburen onshore salt diapir (Groningen Platform) and the M05-2 and M08 offshore salt diapirs (Ameland Platform) using high-resolution datasets integrated with 97 wells. Results indicate that the Pieterburen diapir has progressed to a mature piercement stage, evidenced by the physical truncation of Triassic (Germanic Trias Group) and Cretaceous (Rijnland and Chalk Groups) strata which exhibit sharp upward dragging along the sub-vertical flanks. The crest of Pieterburen lies at a depth of 200m underneath the subsurface. The high-amplitude internal reflectors identified near the base and flanks of Pieterburen and M08 are interpreted as Zechstein floaters, which are brittle anhydrite and carbonate rafts that ruptured during the Hardegsen extensional phase. The offshore M08 diapir has a relatively thicker caprock (57m) than M05-2 (37m). The thickness discrepancy between M08 and M05-2 is driven by the shallower crest of M08 (750m), which increased exposure to meteoric recharge and active subrosion compared to the deeper, more isolated M05-2 (1100m). Additionally, M08 is more heterogenous and has a higher concentration of internal stringers which provides a greater volume of insoluble mineral residue to build a thicker caprock.

Analysis of current repository designs indicates the proposed disposal configuration fits within the boundaries of the studied salt structures. However, the presence of internal impurities and the risks associated with active subrosion necessitate further site-specific research before construction of a facility is possible.

Contents

1. Introduction

The safe, long-term management of high-level radioactive waste is a geo-environmental challenge that many countries in Europe face in the next few decades. In the Netherlands, radioactive waste is currently stored in surface facilities at the Central Organization for Radioactive Waste (COVRA) in Zeeland. Storage is however temporary, and the current recognized approach to long-term isolation and confinement is disposal in a geological disposal facility (GDF) constructed in a stable geological environment beneath Earth's surface. To protect public health and the environment, these repositories utilize a multi-barrier system designed to isolate the radioactive waste from the biosphere (Fig. 1).

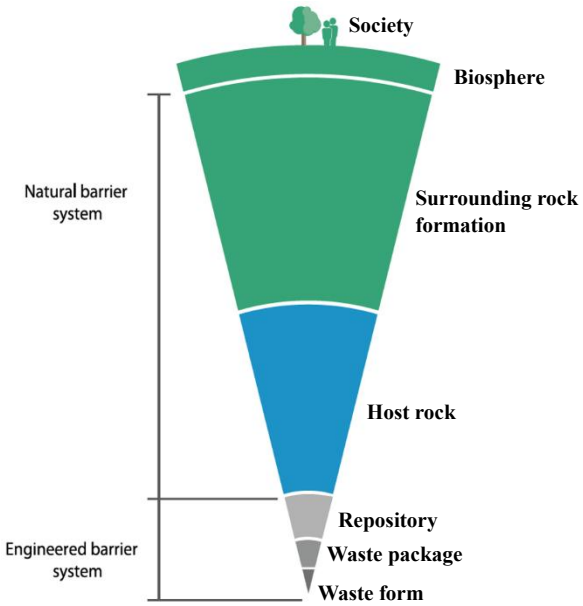

Figure 1: The main components of the natural barrier system and engineered barrier system. Source: Copera Salt, J. Bartol, 2024

One option currently considered in the Netherlands is disposal in domal salt. These evaporite sequences exhibit near-zero permeability and porosity, effectively eliminating advective transport of radionuclides (Cosenza et al., 1999). A geomechanical advantage of salt is its creep behaviour, which allows the rock to seal fractures and voids under lithostatic pressure (Bérest et al., 2023). This ensures a self-healing containment system (Houben et al., 2013; Zeng et al., 2024). Furthermore, rock salt possesses high thermal conductivity, which is essential for dissipating the decay heat generated by high-level waste (HLW) more efficiently than alternative host rocks like clay or granite.

Three salt bodies were studied in this report: The first one being the off shore salt diapir Pieterburen and the two off shore salt diapirs M08 and M05-1. The Pieterburen salt diapir is located on the Groningen Platform in the Northern part of the Netherlands (Fig. 2). The top of the salt diapir lies approximately 200 meters deep, which makes this one of the shallowest diapirs in North of the Netherlands (TNO, 2014). It has a very thick caprock of approximately 90m (Auzemery et al., 2025). The off shore diapirs M08 and M05-2 are situated on the Ameland Platform right above the Terschelling and Ameland (Fig. 2). Other off shore salt diapirs studied in this area show relatively thinner caprock (10-20m) and contain more internal non salt bodies compared to the on shore salt bodies in the North of the Netherlands (Auzemery et al., 2025).

To get a better understanding of the halotectonic behaviours of the Pieterburen, M08 and M05-2 salt diapirs, this study is focused on refining the structural 3D models of the selected onshore and offshore salt diapirs. To achieve this, the Petrel software will be utilized to integrate and interpret high-resolution 2D and 3D seismic reflection datasets. Furthermore, public geoscientific resources from the NLOG will be used to incorporate well-log data and stratigraphic markers, which ensures the refined geometries to be validated against established lithological constraints. These models then get evaluated on the Zechstein salt evolution and their internal structures. Comparison will be reviewed with TNO on the salt geometry and caprock.

2. Geological background

The geological evolution of the Netherlands has resulted in a highly structured and diverse subsurface geology, shaped by various compression and extensional events. The internal structures of the region was primarily influenced by four major tectonic phases: the Paleozoic Caledonian orogeny (orogeny driven by the closure of the Iapetus Ocean (Gee et al., 2013)), the Variscan orogeny (assembly of the Pangea supercontinent), the Mesozoic rifting phases (break-up of Pangea) and the Alpine inversion during the late Cretaceous and Paleogene (de Jager et al., 2025). The study area (Fig. 2) lies on the Groningen and Ameland Platforms and they are situated on the northeastern margin of the Avalonia microplate within the extensive southern Permian Basin. The major tectonic events that affected the study area include the Caledonian and Variscan orogenies, Permian thermal subsidence and salt deposition, Mesozoic rifting during the breakup of Pangea, and Alpine inversion.

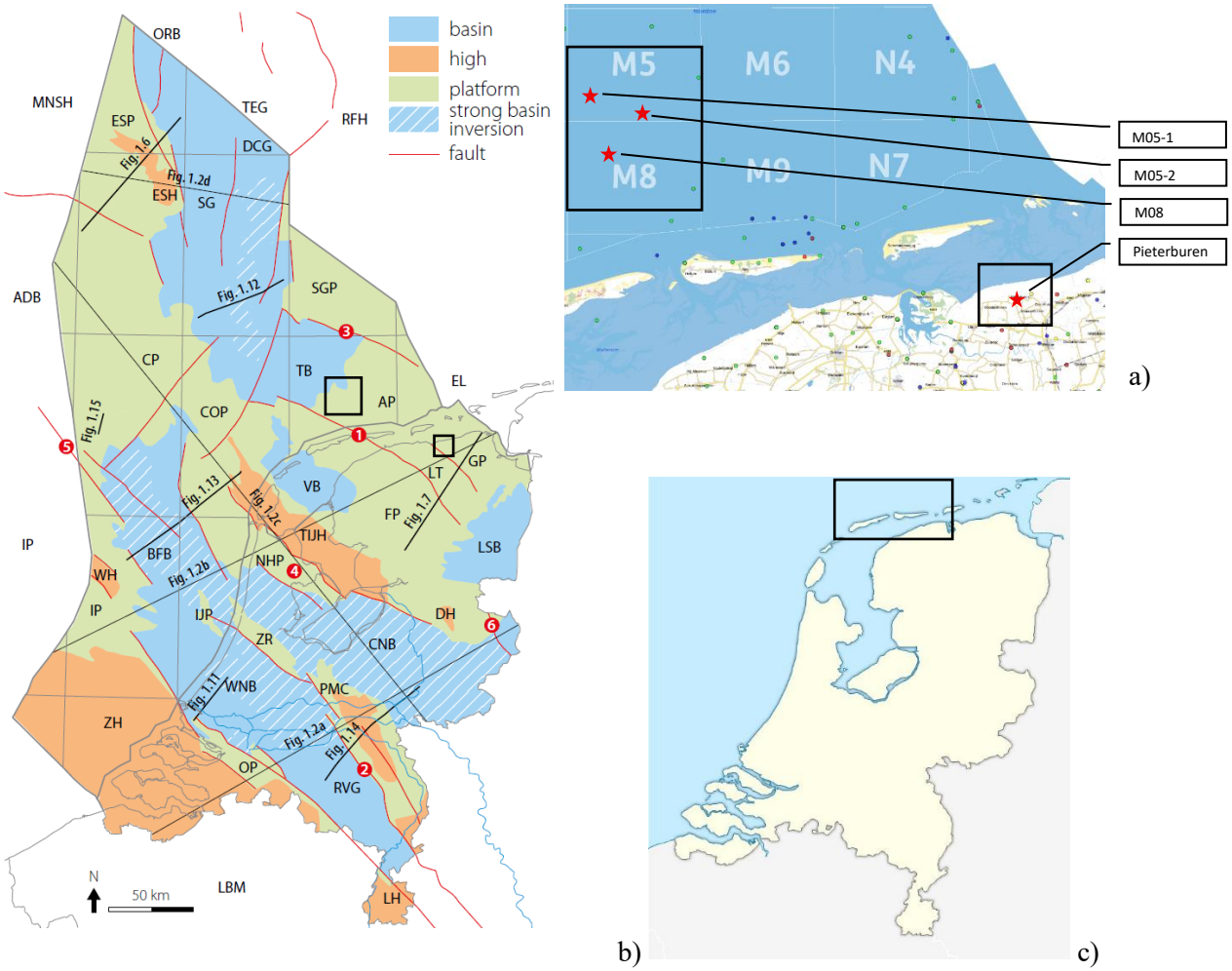

Figure 2 (a-b): a) Location of the salt diapirs within the M block and N block. b) Displays all basins, highs and platforms, this study area is located on the Amersfoort Platform (AP) and Groningen Platform (GP). c) Entire study area of all the studied salt diapirs.

2.1 Permian: deposition of salt

The onset of the Zechstein salt begins at the end of the Permian period, when the Earth's landmasses were united in the supercontinent Pangea. At that time, the area that is now Europe lay about 10° to 20° north of the equator. The regional climate was arid, shielded from the moist air masses by the Variscan mountain range to the south. This created a climate similar to the modern-day Sahara. The southern Permian basin was a vast depression stretching from present-day Poland to England. Because large parts of this basin lay below sea level, a massive marine transgression occurred (Geluk, 2010). Seawater from the northern oceans flooded the area, which created an inland sea. The resulting salt deposits were not a product of a single event but multiple floodings. However, when the connection to the northern ocean was periodically restricted or completely severed through several active faults, the formation of massive evaporite deposits were left behind. This large amount of Zechstein salt was established by five primary evaporitic cycles, denoted Z1 through Z5 (Geluk, 2010). Each cycle represents a progressive increase in salinity followed by a new marine influx (Pichat, 2022). In the central portions of the basin, the upper cycles are significantly thinner and less laterally extensive than the primary Z1, Z2, and Z3 sequences (Zhang et al., 2013).

2.2 Triassic: mobilisation of salt

The transition from the Permian to the Triassic marked the shift from passive evaporite accumulation to active tectonic redistribution. By the Early Triassic (Buntsandstein), regional extension associated with the initial breakup of Pangaea began to affect the Southern Permian Basin (Maystrenko et al., 2013). This extension was primarily oriented East-West and served as the trigger for the first significant phase of halokinesis (Bouroullec et al., 2018; Geluk, 1999). Further mobilization of salt occurred during the mid Triassic as it was triggered by the Hardegsen phase of extensional tectonics (Geluk & Röhling, 1997). This rifting pulse, which was also accompanied by the initial stages of the breaking up of the supercontinent Pangea, provided the structural stress necessary to begin shifting the salt. Tectonic movements transitioned into rift-raft tectonics, which particularly occurred in the Dutch Central Graben (PENGE et al., 1999). This involved the salt acting as a detachment layer allowing the overlying brittle rocks to break into rafts and slide or fault independently. Salt deformation reached its peak during the Late Triassic (Carnian). In the offshore areas north of the Groningen Platform, the Early Triassic was characterized by the development of isolated minibasins (Karlo et al., 2014). As Buntsandstein sediments (Lower Germanic Trias Group) were deposited, they formed a package of relatively uniform thickness, but subsequent extension led to the development of listric faults that soled out into the Zechstein salt (Jager, 2012). These faults allowed the salt to migrate laterally, forming salt pillows and early diapirism structures in the offshore sectors like the Ameland Platform and the adjacent Terschelling Basin (Zhang et al., 2013). Also the onshore Pieterburen area, the salt began to migrate laterally, forming low relief salt pillows (Back et al., 2022). This was likely triggered by the reactivation of older basement faults in the underburden (Li et al., 2024).

2.3 Jurassic: salt withdrawal

The Jurassic period, specifically the Late Kimmerian rift phase, represented the most intensive period of tectonic activity in the North Sea region. This phase was characterized by massive crustal extension, which established the primary rift basins of the Netherlands, including the Dutch Central Graben, the Terschelling Basin, and the Broad Fourteens Basin (Bouroullec et al., 2018). As rifting accelerated in the Dutch Central Graben, the Zechstein salt was actively remobilized into large diapiric structures and salt walls (Bouroullec et al., 2018). The migration of salt out of the areas adjacent to the rifts created rim synclines, where broad depressions created accommodation space for syn-rift sediments of the Schieland and Scruff groups to settle down and exceed thicknesses of over 2,000 meters (Bouroullec et al., 2018; Geluk, 2005). These rim synclines were often filled with siliciclastic non-marine to marginal marine

sediments, reflecting the localized subsidence driven by salt withdrawal rather than regional crustal thinning alone (Roel, 2025). Throughout the Jurassic, the salt continued forming a widespread network of diapirs and pillows that influenced the varying thickness of the Altena Group (Alexandre & Wong, 2025).

While the central rifts of the North Sea were experiencing peak halokinesis, the Groningen Platform was relatively quiet (Li et al., 2024). The lack of significant thickness variations in Jurassic sediments across the platform suggests that the salt at Pieterburen remained in a state of relative equilibrium (Veen et al., 2012).

2.4 Late Cretaceous: inversion

During the Late Cretaceous, the previous extensional regime and post-rift thermal subsidence transitioned into a compressional regime characterised by the Sub-Hercynian and Laramide inversion phases. For the Zechstein salt, the Late Cretaceous was a period of squeezing (De Jager, 2003). Diapirs and salt walls that had formed during the Jurassic extension were laterally compressed, forcing the salt to rise even more rapidly toward the surface (Almalki, 2023). In the northeastern Netherlands (such as the Groningen Platform), salt migration rates peaked during this time, with some diapirs experiencing net growth rates an order of magnitude higher than during previous phases (Li et al., 2024). The Pieterburen salt transitioned into a piercement diapir, with salt rising rapidly to accommodate the compressive stresses (Back et al., 2022). Growth rates during this peak phase reached approximately 0.01 mm/year (Almalki, 2023). Offshore, salt structures in the M05 and M08 blocks were similarly reactivated, resulting in shortening, asymmetric diapir geometries, and renewed vertical growth (Harding & Huuse, 2015).

2.5 Tertiary: post salt burial

During the Tertiary period, the Zechstein salt continued its halokinetic movement, with active displacements persisting into the Neogene in response to ongoing tectonic activity and sedimentary loading. In areas such as the Central North Sea Graben and the Terschelling Basin. This continuous migration resulted in the formation of salt domes and walls that actively disrupted the lateral continuity of Tertiary sedimentary sequences. Throughout the Cenozoic, the salt reached its maximum depth of burial in many regions of the Netherlands (Verweij, 2003). In its present-day state, the deeply buried salt serves as a primary and highly effective seal for underlying reservoirs. This sealing capacity creates a sharp distinction in the modern hydrodynamic setting between the northern over pressured areas, where the salt is laterally and vertically continuous, and the southern regions where the salt is increasingly clastic and permits pressure dissipation (Verweij, 2003).

3. Methodology

To enhance the structural understanding of the onshore and offshore salt diapirs, the primary objective was to generate detailed 3D subsurface model. The modelling process was executed using Petrel Subsurface Software 2024. The generation of the new structural maps for the salt diapirs involved a systemic, multi-step workflow. The initial step involved the interpretation of the seismic subsurface data for the study areas. The aim was to accurately delineate the margins of the salt diapirs and also to differentiate the various stratigraphic layers. Once the seismic interpretation was finalized, a collection of salt diapir maps were constructed. This included a 3D structural model of the salt diapir and isopach maps of the study areas. Finally, the newly created structural diapir maps were subjected to a validation

process involving a comparative analysis against existing diapir maps, which are sourced from the TNO subsurface data centre (DGM-deep) to assess consistency and agreement.

3.1 Seismic interpretation

The construction and differentiation of the stratigraphic layers and salt margins for both the offshore and onshore areas utilized two primary seismic surveys acquired from the TNO data centre. Specifically, the onshore (Pieterburen) salt diapir data was labelled as 'R3137_D_d1k-zo-friesland15-zomdtc-00001' (located within the N-block), and the offshore salt diapir data was labelled 'M05M08_Z3NAM1996A' (located within the M-block). Polygons were delineated around the specific offshore and onshore study areas, which focused the subsequent analysis solely on the region of interest, rather than the entire seismic map extent. Stratigraphic layers were established through the process of well tie, linking specific seismic reflectors that intersect with a borehole where the layer its true stratigraphic position is known from well data. This identified seismic reflector was then traced across the entire seismic survey, either manually or automatically. This process was executed for all required stratigraphic layers, focusing exclusively on tracing the base of each layer. For strong seismic reflectors, such as the Rotliegend, the auto-tracing feature was predominantly utilized due to the clarity of the reflections, while weaker or less clearly visible reflectors needed manual tracing. It is important to note the correlation: the base of the Lower Germanic Triassic (RB) horizon corresponds directly to the top of the Zechstein layer. A quality control step involved viewing the 3D window to verify that the interpreted stratigraphic layers truly intersected the boreholes, addressing potential false intersections that might appear only in the 2D seismic window. Following the tracing and quality control, evenly spaced lines (traced lines on the time slice) were created with an increment of 25 steps for most stratigraphic layers, while the top of the evaporitic Zechstein salt layer required more detail and was modelled using a smaller increment of 10 steps. A total of 788 lines were traced along the time slices of the onshore and offshore study areas. A total of 97 wells located in proximity to the salt diapirs were integrated into the interpretation, with the majority of these data points concentrated in the onshore area (87 wells), and only 10 usable wells available for the offshore study area (Fig. 3a and 3b). Using all these lines and well data different surfaces could be created for each stratigraphic layer.

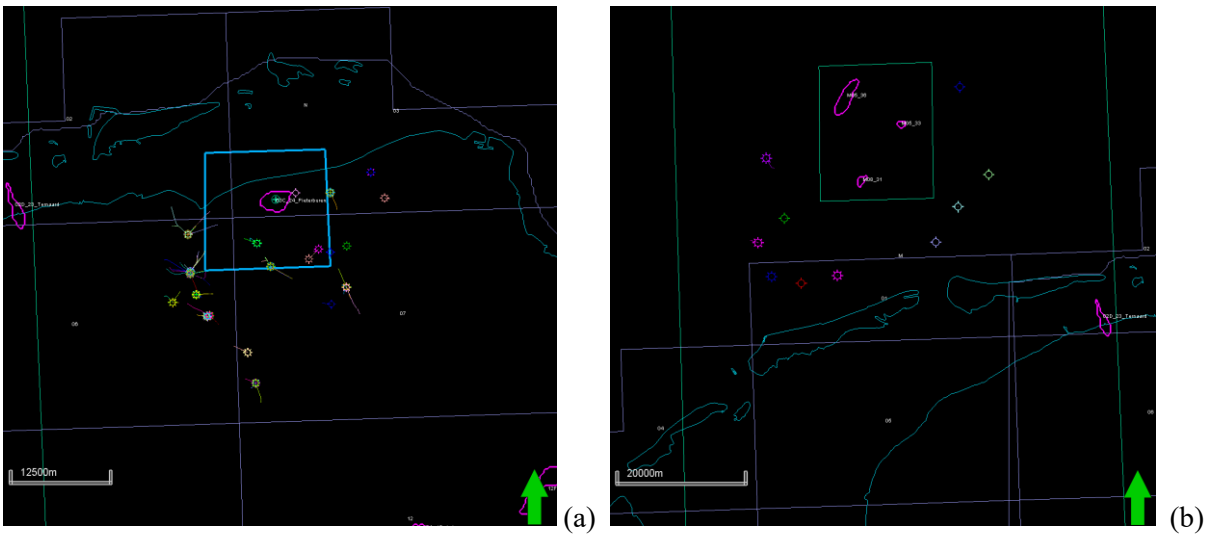

(a) (b)

Figure 3 (a-b): Figure (a) shows all the wells in the grid map for the onshore Pieterburen study area and figure (b) shows all the wells in the grid map for the offshore study area M05-1, M05-2 and M08. The bottom right green arrow shows North direction.

3.2 TWT converting to TVD

While the onshore seismic survey was already calibrated in True Vertical Depth (TVD), the offshore seismic survey was originally provided in Two-Way Travel Time (TWT). Conversely, TVD converts this travel time into actual spatial depth below the surface or sea level by incorporating velocity information, which provides a true measure of structural elevation. Thus, the offshore surfaces created in the TWT domain required conversion to TVD. This conversion was performed using the domain conversion feature within the software, specifically utilizing the 'Velmod_4b_Vint' velocity model to transform the surfaces from TWT into TVD. This model was used because its primary application is time-depth conversion for large scale seismic interpretation and mapping. The Velmod-4b model also outperforms the older Velmod 3.1 model in thickness predictions for the different stratigraphic layers (Doornenbal, 2020).

3.3 Maps

For both the onshore and offshore study areas, multiple subsurface representations were generated, including a 3D structural map of the salt diapirs, alongside 2D isopach maps. To ensure the focus remained strictly on the areas of investigation, main polygons were utilized to define and limit the designated study boundaries. Furthermore, in the offshore area, smaller polygons were created to specifically target the salt diapir peaks situated at depths of 1200 meters or less. This depth constraint was applied because the primary interest of the study lies exclusively in the subsurface volume positioned above the 1200m depth. The generated maps were optimized for relevance by adjusting their visualization starting point to 1200m deep, rather than the base of the entire Zechstein salt layer. This targeted analysis was achieved through the application of the arithmetic operation feature within the modelling software. This operation calculated and created new maps by selecting and isolating only those areas where the salt diapir peaks were positioned above the -1200m. This focusses on the subsequent analysis on the shallowest, most relevant portion of the diapiric structures.

4. Results

Subsurface salt dome analysis was initiated through the seismic mapping of eight distinct reflectors. These reflectors were tied to regional stratigraphic sequences using established well-top markers. For a visual representation of these correlations, see Table 1. The results on the Pieterburen, M05-2 and M08 will be discussed and further analysed. M05-1 is excluded for further analysation because it does not exceeds above 1200m depth, which was mandatory for this study. See appendix for all unedited figures.

Table 1: Seismic reflectors with the corresponding unit and their geological importance. Yellow dashed line traces the reflector that corresponds to the correct unit.

Horizon		Reflector characteristics	Geological importance
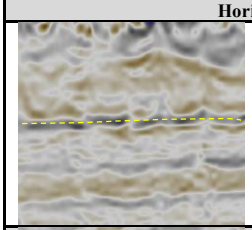	Base Upper North Sea Group (NU)	Very weak to weak, seems to be continuous but displays a lot of wavy artifacts	Mid-Miocene Unconformity (Huuse & Clausen, 2001)
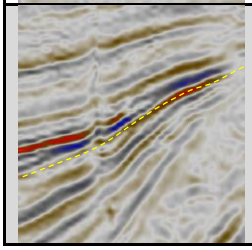	Base Middle North Sea Group (NM)	Weak to medium reflectors and is continuous	Early Eocene to Oligocene transition

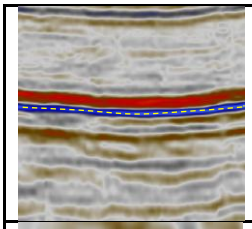	Base Lower North Sea Group (NL)	Very strong reflector and is continuous	Erosion of Chalk and Laramide inversion (Duin et al., 2006)
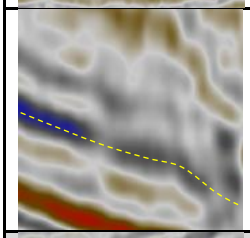	Base Chalk Group (CK)	Medium to high dispersed reflector and is continuous	Depositional change, from marl to chalk (Lauwerier, 2022)
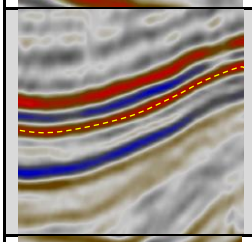	Base Rijnland Group (KN)	Medium to strong reflector and is continuous	Late Cimmerian tectonic phase, Base Cretaceous unconformity (Duin et al., 2006)
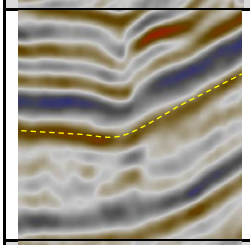	Base Upper Germanic Trias Group (RN)	Medium reflector and is continuous	Triassic erosional boundary caused by regional tectonic tilting and sea level change, Hardegsen Unconformity (Filomena & Stollhofen, 2011)
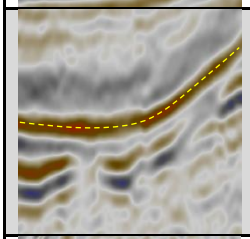	Base Lower Germanic Trias Group (RB)	Medium to strong appearance. Strong reflection if it overlays ‘floaters’ (evaporites banks inside the salt)	Top salt
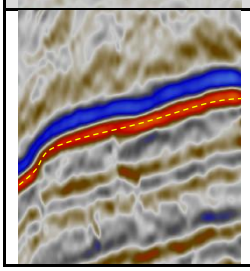	Base Zechstein Group (ZE)	Has a very strong reflector. Continuous away from salt diapir, but discontinuous near salt diapir	Permian subsalt basement

4.1 Seismic Interpretation: On-shore Pieterburen Salt Diapir

Figure 4 displays a seismic profile of the Pieterburen salt diapir, which is located on the Groningen Platform. A 3D version of the Pieterburen salt diapir is shown in figure 5c. The dashed line in the isopach map (Fig. 5b) indicates the exact orientation of this cross-section. The salt diapir shows a high-relief Zechstein (ZE) salt diapir that originated in the salt layer below 3000m deep. The salt diapir exhibits a maximum thickness of over 3000m in the centre, which reduces to 200m in NW direction toward the Ameland Platform (neon pink, Fig. 5b). The diapir exhibits a sub-vertical geometry characterized by a broad base and a bulbous crest at approximately 300m depth. The crest forms a dome that terminates within the Chalk Group (CK). The lateral margins of the salt body are steeply dipping. The West flank maintains a consistent steep gradient, while the eastern flank displays a secondary salt shoulder at approximately 2000m deep. Extensional crestal faults appear on the eastern overburden (cross cutting

CK, KN and RN) caused by localized stretching of the overburden as the salt diapir arched the overlying strata (Fig. 4).

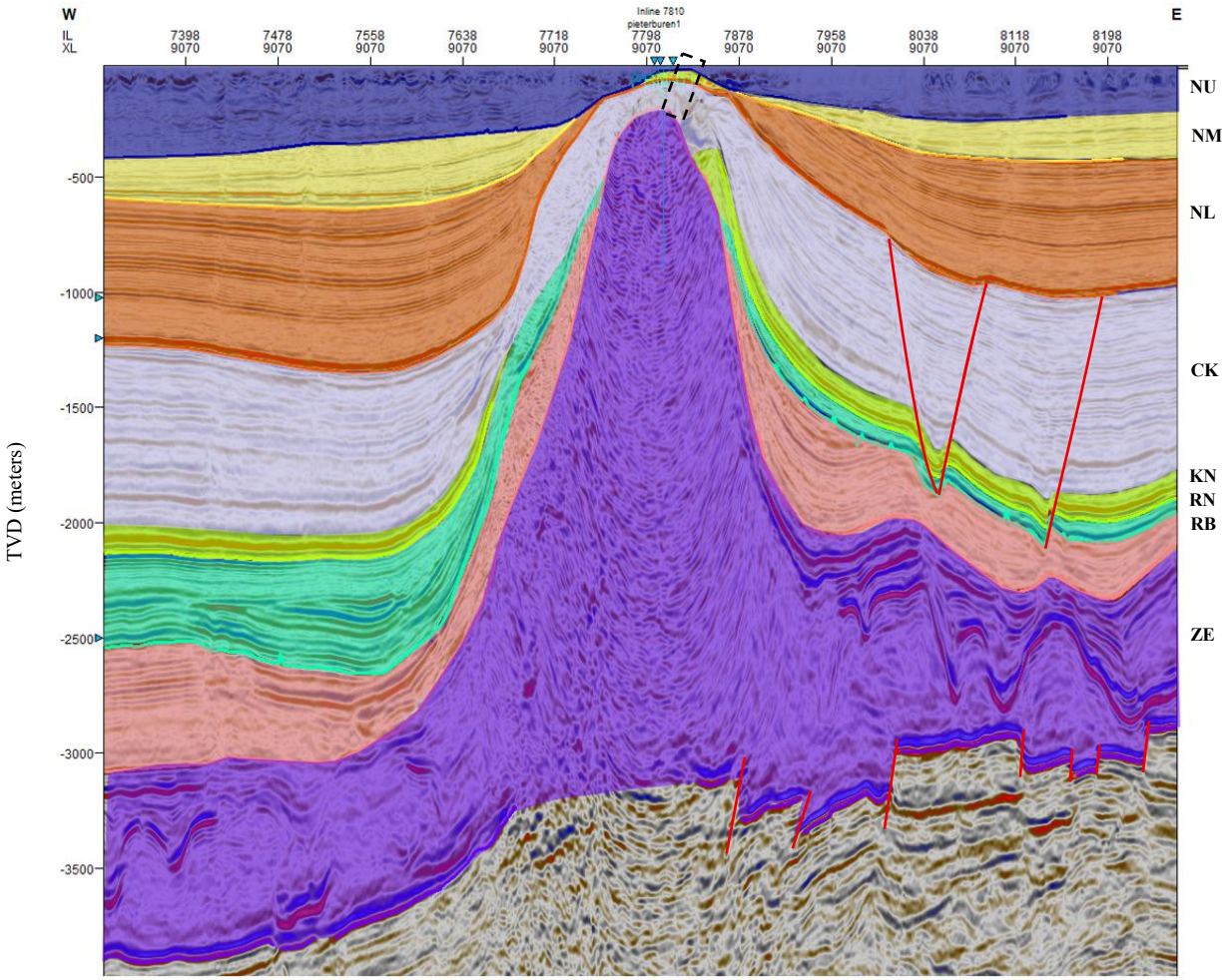

Figure 4: Seismic interpretation of Pieterburen salt diapir, W-E cross section on Xline 9070. Purple (ZE), pink (RB), light blue (RN), green (KN), grey (CK), orange (NL), yellow (NM), navy blue (NU). Y-vertical is depth in meters, X-horizontal is Inline/Xline. The black dashed rectangle shows the thinned strata of CK, NL, NM and NU.

The RB, RN and KN layers at the base are physically truncated and rotated nearly vertical. This indicates that the salt began to move upward shortly after these sediments were deposited. The steep drag and rotation suggest an active piercement phase, where regional extension likely cracked the overburden, allowing the pressurized Zechstein salt to push through. There is an unconformity between the KN group and the CK group at the crest of the salt where the CK group is in direct contact with the Zechstein salt. The Triassic units do not drape over the salt, they stop abruptly against its margins. Which indicates the active piercement phase of the salt diapir. the salt was a topographic high on the seafloor. Sediment was deposited around it but the salt was rising faster than the sediment could cover it.

Stratigraphic thinning observed in the CK, NL, NM, and NU groups (Fig. 4) confirms that the primary phase of diapirism was initiated in the Late Cretaceous with a high volume salt flux and remained active through the Cenozoic. The continued thinning within the NU demonstrates that halokinesis persisted into the most recent depositional periods, which maintains the crest as a topographic high that restricted accommodation space. However, the transition from truncation in the lower units to a continuous thinned drape in the NU layer indicates a reduction in the relative rate of salt rise. It has reached a near equilibrium state where the salt supply is likely exhausted ore the lithostatic pressure of the overburden has equalized with the buoyancy of salt. This shifts a stage of piercement phase toward a diminishing stage of draped growth.

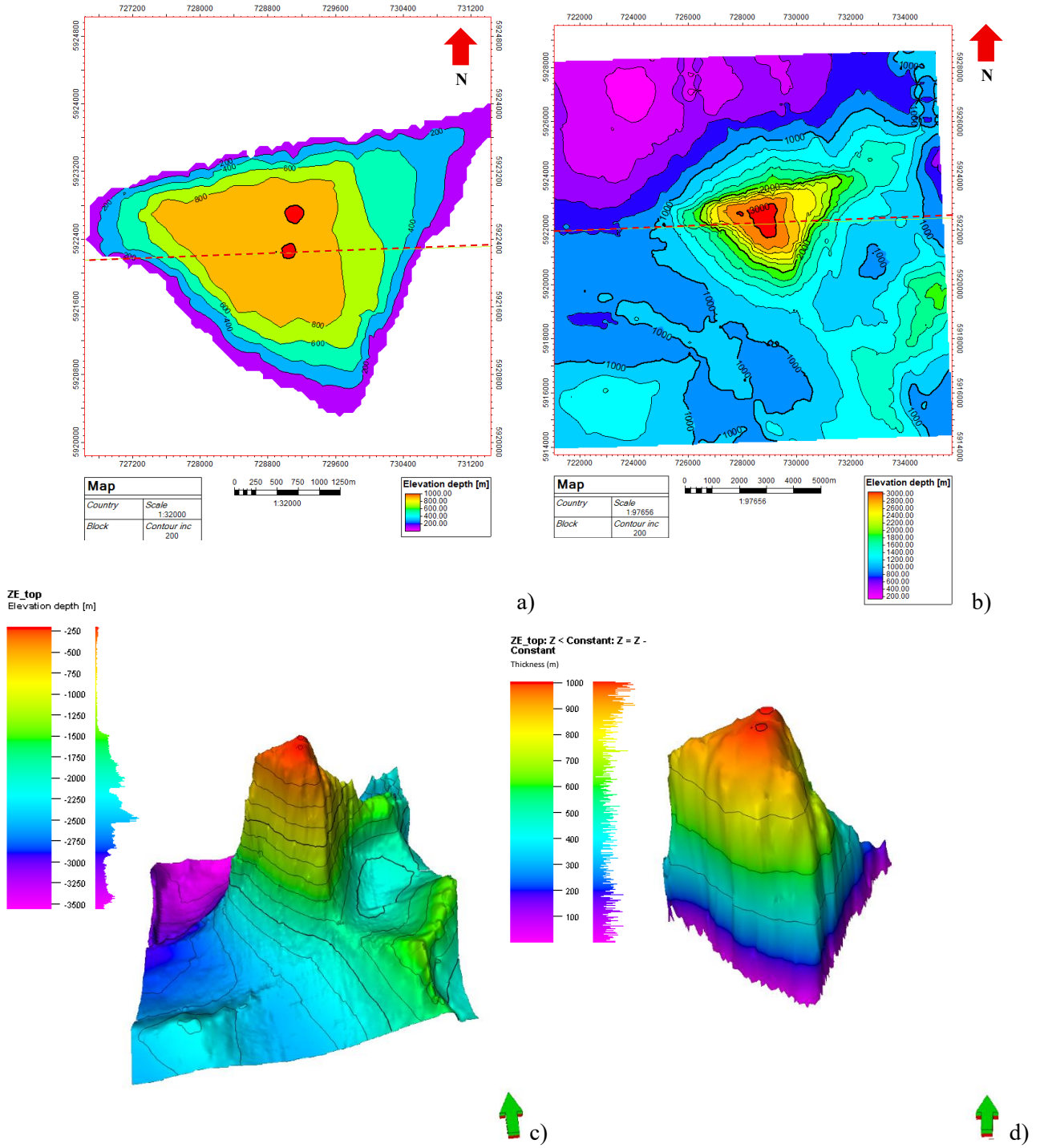

Figure 5 (a-d): a) Isopach map with 200m increments, the thickness measurement starts at a depth of 1200m deep, which is seen as thickness 0m. Red dashed line shows the exact orientation of the Pieterburen salt diapir cross section. b) Total thickness map of the Pieterburen salt, measuring from the base towards the top of the Zechstein salt. c) 3D map of the Pieterburen salt diapir. d) 3D map of only the top section starting from a depth of 1200m (the green arrow on the bottom right represents North).

Figure 5a illustrates the thickness distribution of the Pieterburen salt diapir above a base depth of 1200m. The salt body exhibits a concentrated, sub-triangular depocenter. Thickness values ranges from a marginal 200m to a localized maximum exceeding 1000m. The peak thickness corresponds to the diapir crest, which reaches a minimum depth of 200m below the subsurface. Contour intervals are set at 200m,

revealing a steep thickness gradient along the N and SW margins. This spatial arrangement indicates a rapid transition from the salt rock to the surrounding host rock. A 3D version can be seen in figure 5d.

The orange area has a thickness of approximately 800m at a burial depth of 400m. It has a maximum lateral width exceeding 2400m along NW-SE axis. Within this zone, two distinct red circular anomalies indicates the highest vertical relief of the structure, where salt thickness surpasses 1000m. The asymmetry of the map (the elongated purple tail extending toward the NE) suggests a preferential direction of salt flow or an underlying structural control. The convergence of contours toward the boundaries reflects the sub-vertical geometry of the flanks observed in seismic sections.

4.1.1 Internal salt structures

The Pieterburen salt diapir exhibits a transition from a homogeneous halite core to heterogeneous internal structures. The central region of the body is characterized by seismic transparency, indicating a uniform composition of halite that lacks internal acoustic impedance contrasts. This homogeneity is interrupted near the base and along the steep flanks by high-amplitude, discontinuous reflectors (Fig. 6). These features represent intrasalt floaters, primarily composed of brittle anhydrite and carbonate layers. These brittle layers of anhydrite and carbonate do not flow as easily as halite. The layers rupture and float within the salt as rafts, where they rotate and fold during the vertical ascent of the salt. They represent the tectonic fragmentation of the Zechstein 2 (Stassfurt) or Zechstein 3 (Leine) carbonate and anhydrite layers (Geluk, 2010; Remmelts, 2011). Wellbore PBN-01 at Pieterburen provides data down to a depth of 900m (Remmelts, 2011). The interval between 300 and 780 m consists of halite (Z3). From 780 to 810 m, the lithology becomes heterogeneous, comprising halite, anhydrite, carbonate, and claystone (TNO, 2014). Below this, from 810 to 900 m, the succession returns to homogeneous halite, with intervals of anhydrite floaters (Z2). On top of the Z3 salt, there resides a caprock in between 315-220 deep which is approximately 100m thick (TNO, 2014). The pure massive halite Z2 sequence of the Zechstein begins at the 900m depth, but this is also the maximum penetration depth that the borehole drilled in to (Remmelts, 2011). Further exploration drilling deeper into the Zechstein salt on PBN-01 well is required to reconstruct the genetic evolution of the Zechstein cycles.

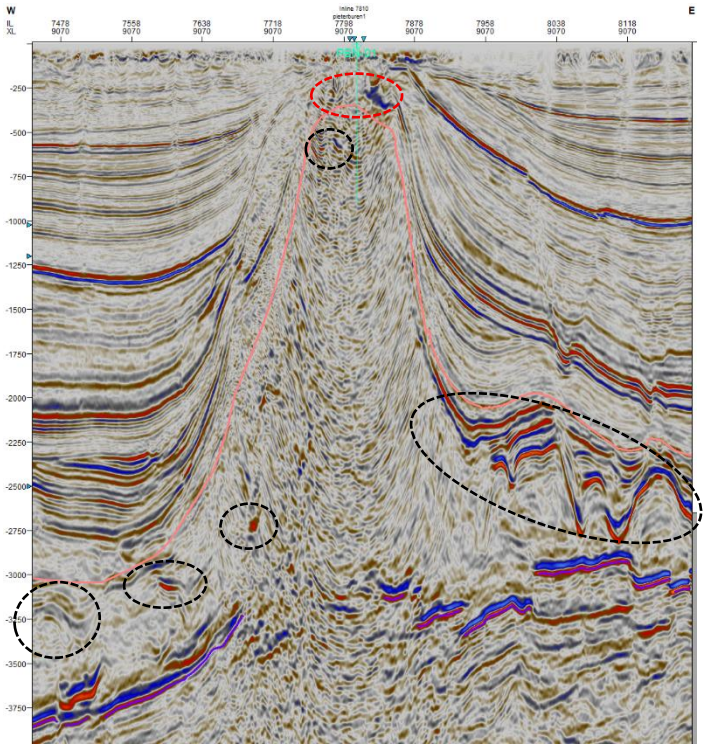

Figure 6: Internal salt structures of carbonate and anhydrite floaters are circled in black. Caprock on top is circled in red

In figure 6, the caprock resides outside the salt body, forming a structural interface between the salt crest and the overlying sedimentary overburden. It is located at 350-200m deep (approximately 150m thick caprock). Unlike the wavy or folded internal floaters, the caprock displays high seismic reflectance and a chaotic, discontinuous texture. This high reflectance is a product of the high acoustic impedance contrast between the dense caprock minerals and the lower-velocity sedimentary overburden or the salt below. The caprock is marked with a red circle (Fig. 6).

4.1.2 Comparison with TNO

The cross-section extracted from the TNO model does not correspond to an identical spatial location as the seismic interpretation due to coordinate system discrepancies between Petrel and DINOloket. The alignment was performed visually, trying to achieve the closest possible approximation.

Both interpretations identify a salt diapir originating from the top of the Zechstein Group at a depth of approximately -3050m (Fig. 7) . The general morphology of the structure is consistent across both datasets, characterized by a vertical salt piercement that truncates the surrounding sedimentary sequences including the Germanic Trias, Rijnland, and Chalk groups. The lateral extent and the slope of the western flank show a high degree of correlation between the two models. The eastern side also show close correlation but the two smaller shoulder peaks seem to shift a little bit to the west compared to the results of this study.

Differences are primarily observed in the vertical relief and the specific geometry of the salt crest. The seismic interpretation results in a salt top elevation of -180m, whereas the TNO model places this boundary at -600m. The seismic-derived surface displays a narrower and more pointed crest compared to the broader, more rounded profile presented by TNO. Furthermore, the RN group seems to absent on the east side of the diapir.

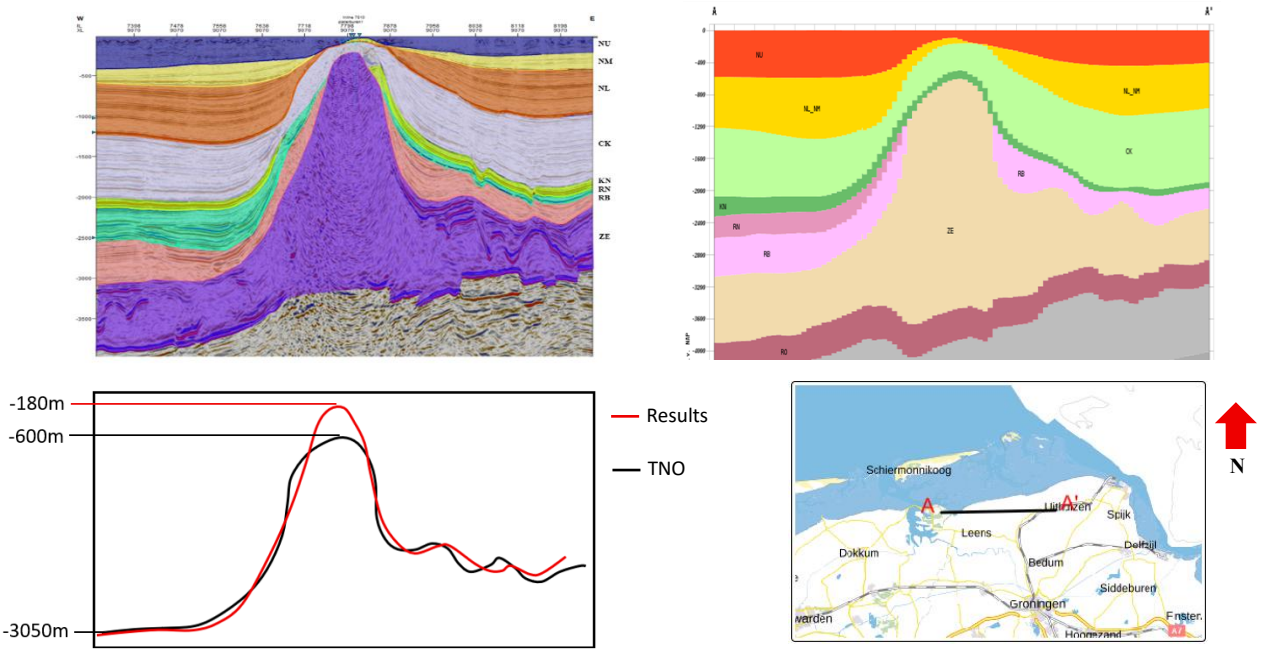

Figure 7: Comparison of interpreted salt diapir geometry between seismic results (top left) and the TNO model (top right). The bottom left plot highlights structural deviations, specifically the crestal depth difference (-180m vs -600m). The cross-section is taken from DINOloket and its location is from West – East, respectively A-A'(bottom right). Red arrow indicates North.

4.2 Seismic Interpretation: Off-shore Salt diapirs

M05-2

Figure 8 displays a seismic profile of the off-shore salt diapir (M05-2, residing in the M05-block), which is located on the Ameland Platform. A 3D version of the off-shore salt diapir is shown in figure 9c. The red dashed line in the isopach map (Fig. 9a) indicates the exact orientation of this cross section. The salt body has a basin floor of 2500m deep and narrows upwards into a crest at approximately 850m depth. The salt diapir is sub-vertical with asymmetrical flanks. The west flank shows a steep linear gradient, while the east flank has a lateral bulge at approximately 1750m depth. The salt thickness has topographic variation (200m-3600m), which indicates salt migration towards the central conduit.

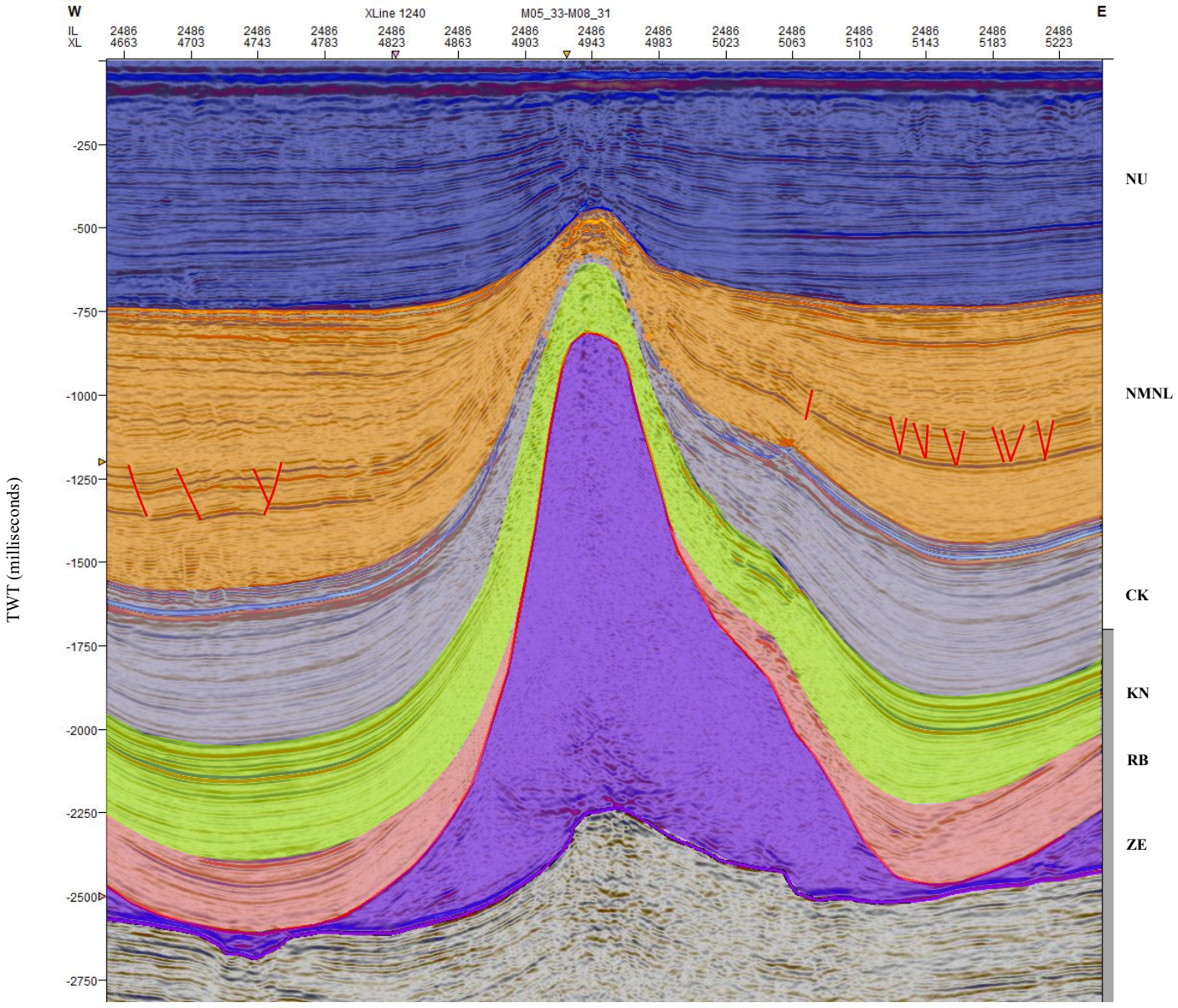

Figure 8: Seismic interpretation of M05-2 salt diapir, W-E cross section on Inline 2486. Purple (ZE), pink (RB), green (KN), grey (CK), orange (NLNM), navy blue (NU). Y-vertical is shown in TWT (ms), X-horizontal is Inline/Xline. The apparent structural high at the base of the Zechstein (ZE) unit is a seismic artifact caused by velocity pull-up.

It is noticed that the RN unit is missing in between the RB and KN unit in this location. The absence of the RN unit indicates a period of non-deposition or localized erosion, possibly driven by early-stage salt-induced uplift before the salt fully breached the surface. The upward migration of the Zechstein salt has fully pierced through the RB unit. Conversely, KN and CK do not experience full piercement of the salt diapir but they exhibit drag folding and upturning along the along the diapir flanks, which transitioned the sub-horizontal orientations to steep dips at the salt diapir contact. This suggests that the total piercement of the RB unit indicates an initial phase of high-rate active diapirism. As the system evolved into the KN and CK intervals, the diapir transitioned into a passive growth phase. The dramatic thinning observed in the NMNL unit represents a pulse of syn-depositional halokinesis, where the rising salt maintained a topographic high, forcing sediment bypass. Lastly, the uniform thickness of the NU unit marks the stagnating movement, where the rate of burial overwhelmed the waning salt supply.

Figure 8 shows a set of synthetic and antithetic faults within the NMNL unit. The faults show relatively small vertical offsets, but they clearly offset the internal reflectors of the NMNL unit. The faults do not cross cut the NU unit which suggest that by the time the NU unit was deposited the salt movement has slowed down or ceased.

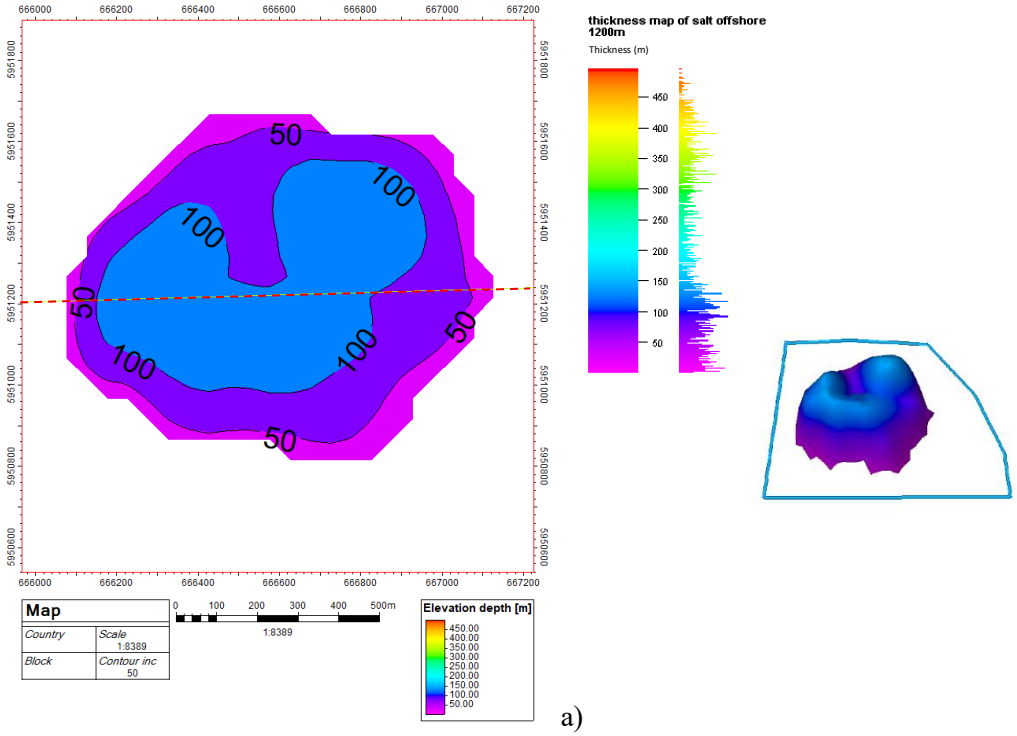

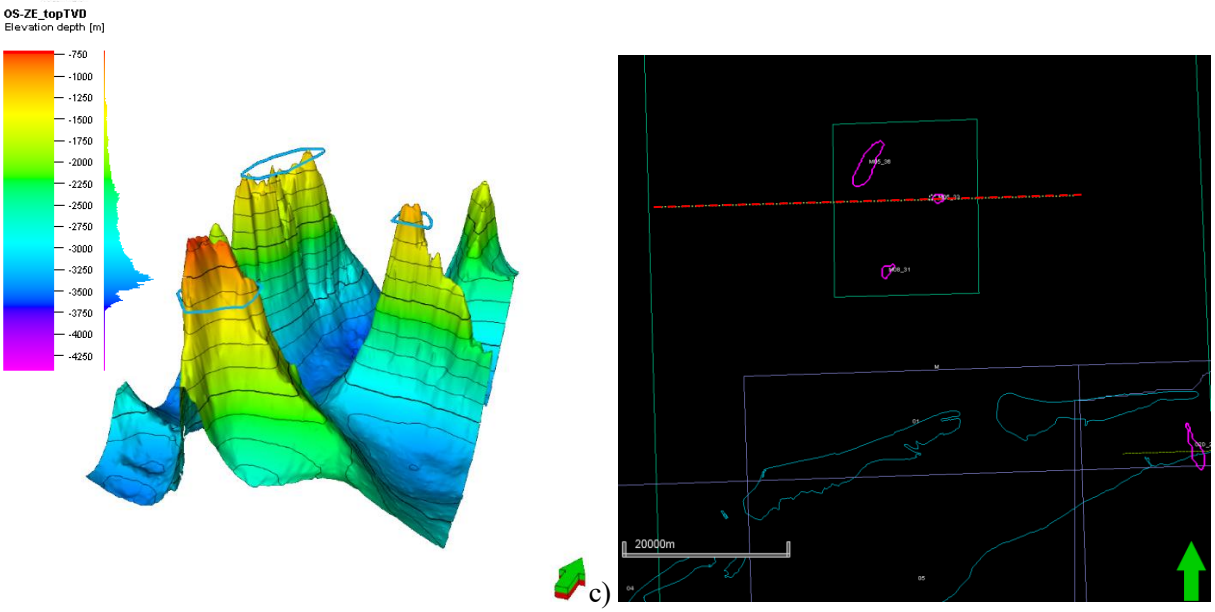

Figure 9 (a-d): a) Isopach map with 200m increments, the thickness measurement starts at a depth of 1200m deep, which is seen as thickness 0m. Red dashed line shows the exact orientation of the M05-2 salt diapir cross section. b) 3D map of only the top section starting from a depth of 1200m. c) 3D map of the M05-2 salt diapir. d) Red dashed line shows the cross section direction in grid map of Petrel, scale is included on the bottom left. Green arrow on the bottom right indicates North direction.

The isopach map of the offshore salt diapir (Fig. 9a) illustrates the spatial distribution of salt thickness above a depth of 1200m. The salt body exhibits a maximum thickness of 100m, coinciding with the diapir's crest at a subsurface depth of 1100m. A 3D version of this isopach map can be seen in figure 9b. The surface of the salt diapir has an irregular structure with a maximum width of 980m. The thickness distribution at the blue surface (the two blue areas enclosed by the 100m contour line) shows a dual-lobed morphology. This lateral variability in thickness reflects the internal complexity of the Zechstein salt.

M08

The second salt diapir (Fig. 10) belongs to the off-shore area within the Ameland Platform, but resides inside the M08 block instead of the M05 block. A 3D version of this diapir is shown in figure 11c. The red dashed line in the isopach map (Fig. 11a) indicate the exact orientation of this seismic cross section. The salt body has a basin floor of approximately 2700m deep and rises up to a narrow crest at 750m deep. The diapir is asymmetric with a steeper western flank compared to a more gradual, draped eastern flank. It is seen that the RN unit is missing in between the RB and KN unit. The RB unit is partially missing in the western flank of the salt and the KN unit shows significant thinning against the western margin of the salt diapir. The RB and KN unit on the eastern flank don't show any thickness variation but are more continuous. The KN and NMNL units exhibit a "drape" or "onlap" geometry against the salt, suggesting that while the salt was rising, the eastern side remained a relative structural low, preserving a thicker sedimentary sequence. The CK unit exhibits a unconformity at the diapir crest, where it is partially to entirely absent. The NMNL unit is very thin and drapes over the high structure. This indicates that the diapir remained a topographic high through the Paleogene. A change in structural style is observed in the NU unit. Unlike the underlying units, the NU maintains a relative consistent thickness across the crest of the diapir. This indicates that by the Neogene, the rate of regional sedimentation exceeds the rate of halokinesis. The thick NU sequence marked the transition from an active, seafloor-piercing diapir to a buried salt body.

Eastern dipping normal faults are seen inside the NMNL unit. These faults are strictly Cenozoic, because they do not cross cut any other units. They formed during the deposition of the NMNL unit because the offset of the internal NMNL reflectors do not appear to displace the upper NU seafloor layers. This means that the brittle deformation of the overburden peaked just before the diapir was finally buried.

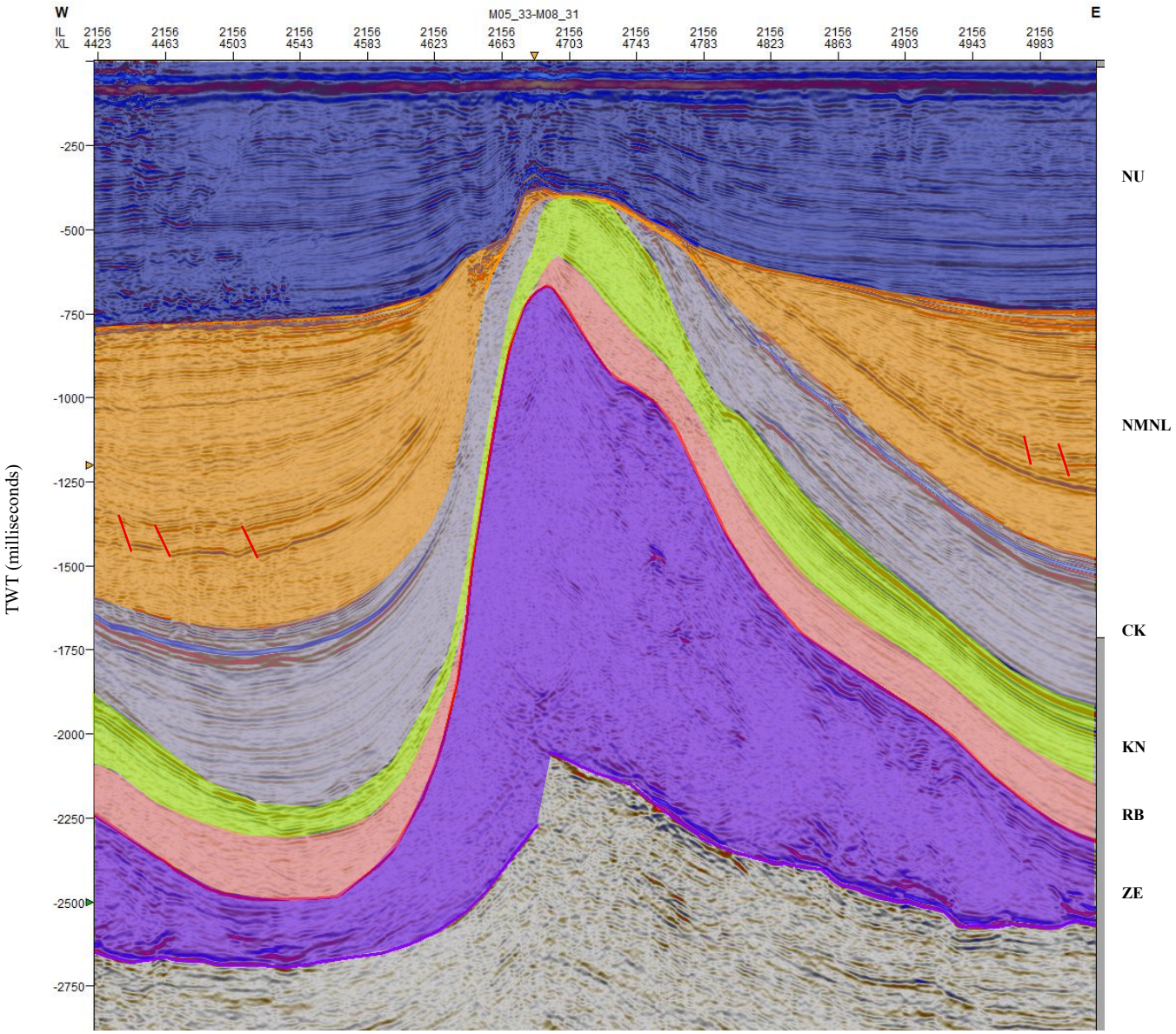

Figure 10: Seismic interpretation of M08 salt diapir, W-E cross section on Inline 2156. Purple (ZE), pink (RB), green (KN), grey (CK), orange (NLNM), navy blue (NU). Y-vertical is shown in TWT, X-horizontal is Inline/Xline. The apparent structural high at the base of the Zechstein (ZE) unit is a seismic artifact caused by velocity pull-up.

The isopach map in Figure 11a reveals an elongated, lobate salt geometry with a northeast-southwest orientation. Above 1200m deep the structure reaches a maximum thickness of 450m in the southwestern region and a minimum thickness of 50m in the purple surface. A central zone with a thickness of 350m and a maximum width of 1260m is located 850m below the subsurface. The contour spacing is tighter along the western margin, indicating a steep structural wall, whereas the eastern margin displays a more gradual thinning and a secondary lobe. This asymmetric distribution of salt thickness suggests that the development of the diapir was influenced by differential sedimentary loading or regional tectonic trends.

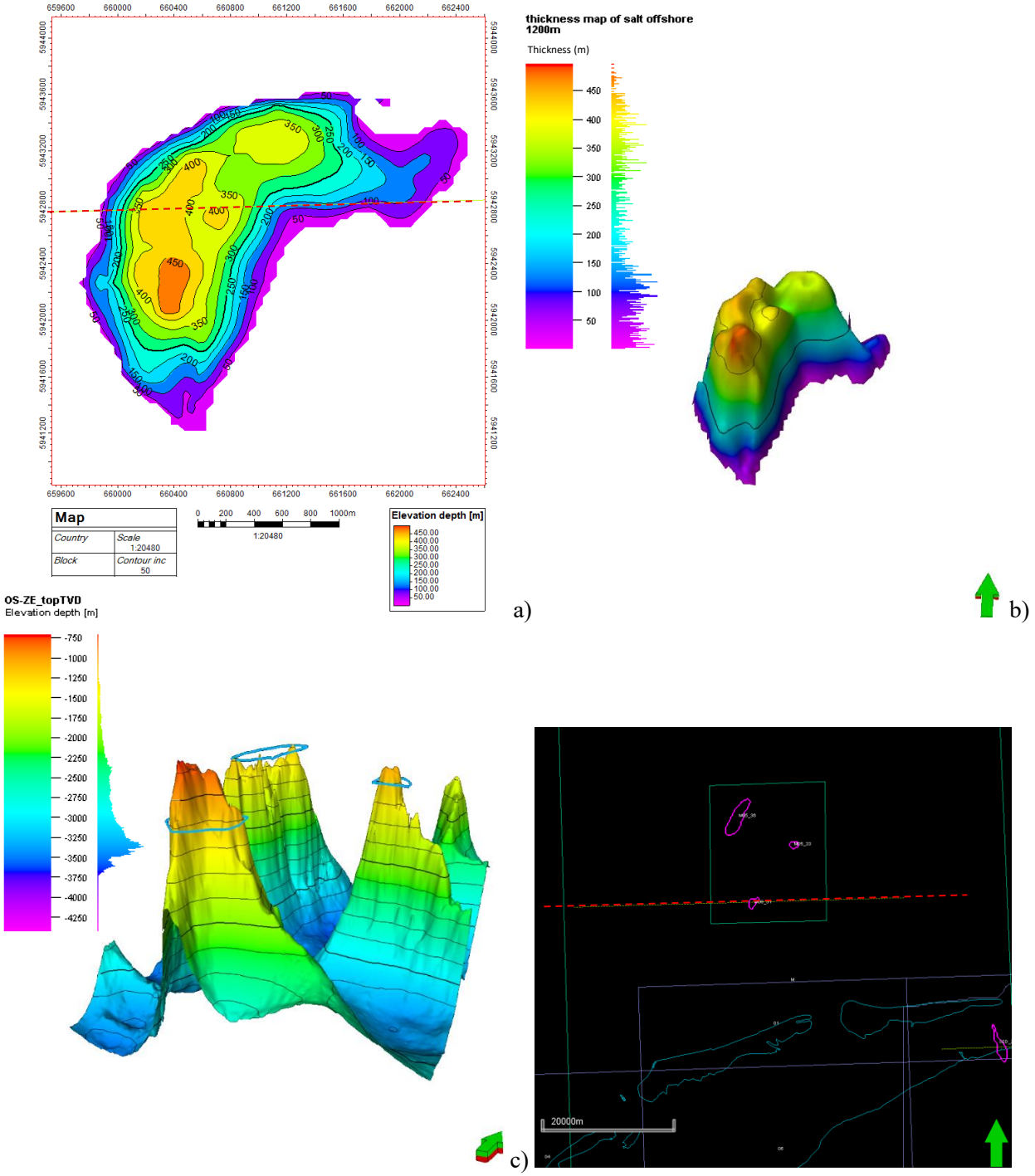

Figure 11 (a-d): a) Isopach map with 200m increments, the thickness measurement starts at a depth of 1200m deep, which is seen as thickness 0m. Red dashed line shows the exact orientation of the M05-2 salt diapir cross section. b) 3D map of only the top section starting from a depth of 1200m. c) 3D map of the M08 salt diapir. d) Red dashed line shows the cross section direction in grid map of Petrel, scale is included on the bottom left.

4.2.1 Internal salt structures

Figure 12a displays the off-shore salt diapir M05-2 and figure 12b displays the off-shore salt diapir M08. M05-2 shows a predominantly transparent seismic facies with faint, discontinuous sub-horizonal reflectors in the core, which suggests high homogeneous halite. There are a few high amplitude fragmented reflectors visible on the base of this salt diapir, which is circled black in figure 12a. In M08, the internal structure contains more stringers (high amplitude fragmented reflectors). They show up as broken up fragments in the centre right side of the salt diapir and appear deformed and folded along the fight flank and the base of the salt diapir (Fig. 12b, circled in black). Therefore, the salt in M05-2 is more homogeneous than in M08. Caprock is present at the crest of both diapirs, they appear as a high-amplitude, chaotic seismic unit above the salt diapir crest (see red circles in Fig. 12). Measuring the thickest point of the caprock (centre), M05-2 has a caprock thickness of approximately 37m, while M08 has a thicker caprock of 57m. The caprock in M08 is much thicker and displays a more chaotic seismic character than in M05-2. This thicker caprock, composed of residual anhydrite and claystone (Auzemery et al., 2025), is directly overlain by a prominent crestal sag in the Cenozoic North Sea Group.

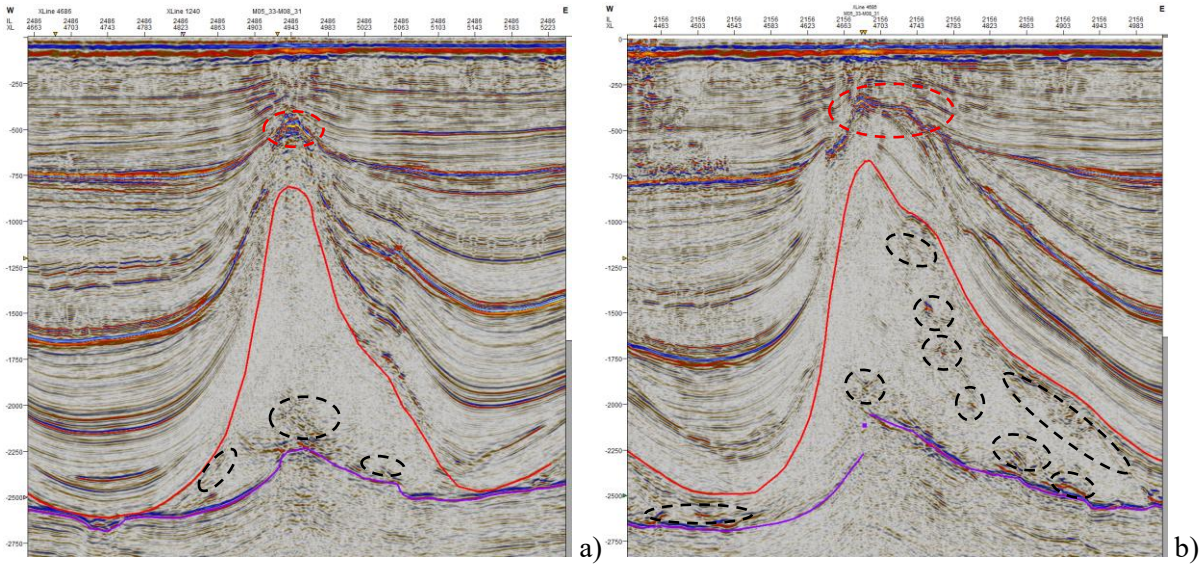

Figure 12(a-b): Red line traces the top of the Zechstein salt and the purple line traces the base of the Zechstein salt. a) M05-2 has a caprock thickness of 37m. b) M08 has a caprock thickness of 57m. Black circles indicate floaters (non-salts within the salt diapir) and the red circles indicate the caprock.

4.2.2 Comparison with TNO

This analysis examines the offshore salt diapir M05-02 and M08, comparing a regional depth-model interpretation extracted from TNO's DINOloket with a seismic interpretation derived from Petrel. The approximate surface location of the cross-section A-A' is shown in the bottom left map (Fig. 13 & 14). A precise spatial overlay between the results of TNO and of this study not attainable due to inherent discrepancies between the coordinate systems utilized in Petrel and the DINOloket database. Furthermore, a direct quantitative comparison of absolute depths, thicknesses, or dips is precluded because the TNO model is presented in True Vertical Depth (meters), whereas the seismic interpretation is displayed in Two-Way Time. Due to velocity variations in the subsurface, particularly the high velocity of salt relative to surrounding sediments, structures in time domains often appear distorted compared to their true depth geometry. Therefore, this comparison focuses solely on the observable differences in structural style, relative geometry, and stratigraphic relationships.

M05-2

Both interpretations identify a mature, fully developed salt diapir originating from the Zechstein Group. The general morphology in both models shows the salt body piercing through the overburden stratigraphy, including the Triassic (RB, KN), Cretaceous (CK), and Tertiary (NM/NL, NU) groups. A common feature is the pronounced upward drag of the sedimentary layers immediately adjacent to the salt flanks, indicating significant halokinetic movement.

Both models identify a high-relief Zechstein salt diapir that has successfully pierced the Triassic RB group. Both geometries of the North Sea groups and Chalk group seem to match each other. The general structural style is consistent, showing a mature piercement structure with significant upward drag and deformation of the surrounding stratigraphic units. Both interpretations indicate that the diapiric movement influenced the entire sedimentary column, reaching close to the seabed. However, the TNO model depicts a more aggressive piercement, where the salt has completely pierced through both the RB and KN group. In contrast, the seismic results show a full piercement only through the RB unit, while the KN unit remains as a continuous drape over the salt flanks. The CK group on the seismic results also seem much thinner compared to the TNO model.

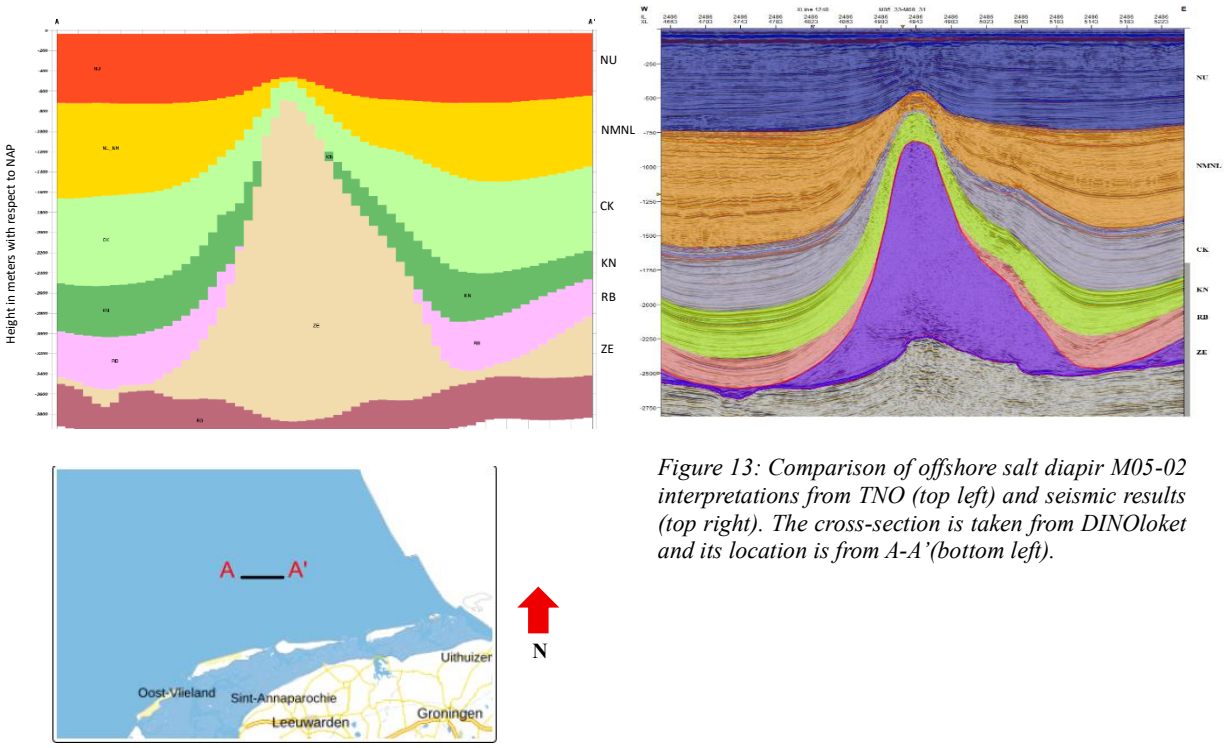

Figure 13: Comparison of offshore salt diapir M05-02 interpretations from TNO (top left) and seismic results (top right). The cross-section is taken from DINOloket and its location is from A-A'(bottom left).

M08

The seismic model looks different from the TNO model. The western flank of the seismic model appears steeper compared to the TNO model. The strata above the salt diapir on TNO model also look more continuous in thickness while the seismic model has a lot of different thicknesses. The RB group seems to be partially absent on the western flank of the diapir. The RB, KN and CK group appears to have a more continuous thickness on the eastern side of the salt diapir while KN and RB group seems to thin towards the flanks of the salt diapir. The Chalk group also seem to be absent above the crest of the diapir and the NMNL group seems thin significantly towards the crest of the salt diapir. Both NU group seem to be similar and seem least influenced by the rising of the salt diapir.

The comparison between the TNO regional framework and the high-resolution seismic interpretation reveals structural and stratigraphic variations. In the seismic model, the western flank of the diapir has a higher inclination gradient than represented in the TNO model. The TNO model depicts the feature with a more symmetrical morphology. While the TNO model shows stratigraphic continuity in thickness across the structure, the seismic interpretation identifies significant thickness variations and truncations. Across both models the RN group is absent, which confirms a period of non-deposition or localized erosion that was possibly driven by early-stage-salt-induced uplift before the salt fully pierced the surface. The RB group displays an absence along the western flank in the seismic model, likely resulting from erosion or tectonic truncation during the piercement phase of the salt. This contrasts with the eastern flank, where the RB, KN, and CK groups show greater preservation and thickness continuity. Both the RB and KN groups exhibit thinning as they approach the salt flanks, which indicate the syn-kinematic deposition during early halokinetic uplift. The seismic data shows the absence of the CK group. Furthermore, the NMNL group undergo significant thinning towards the crest. In contrast, the NU group maintains a relatively uniform thickness in both models, indicating that the rate of salt rising decreased or stabilized by the Neogene.

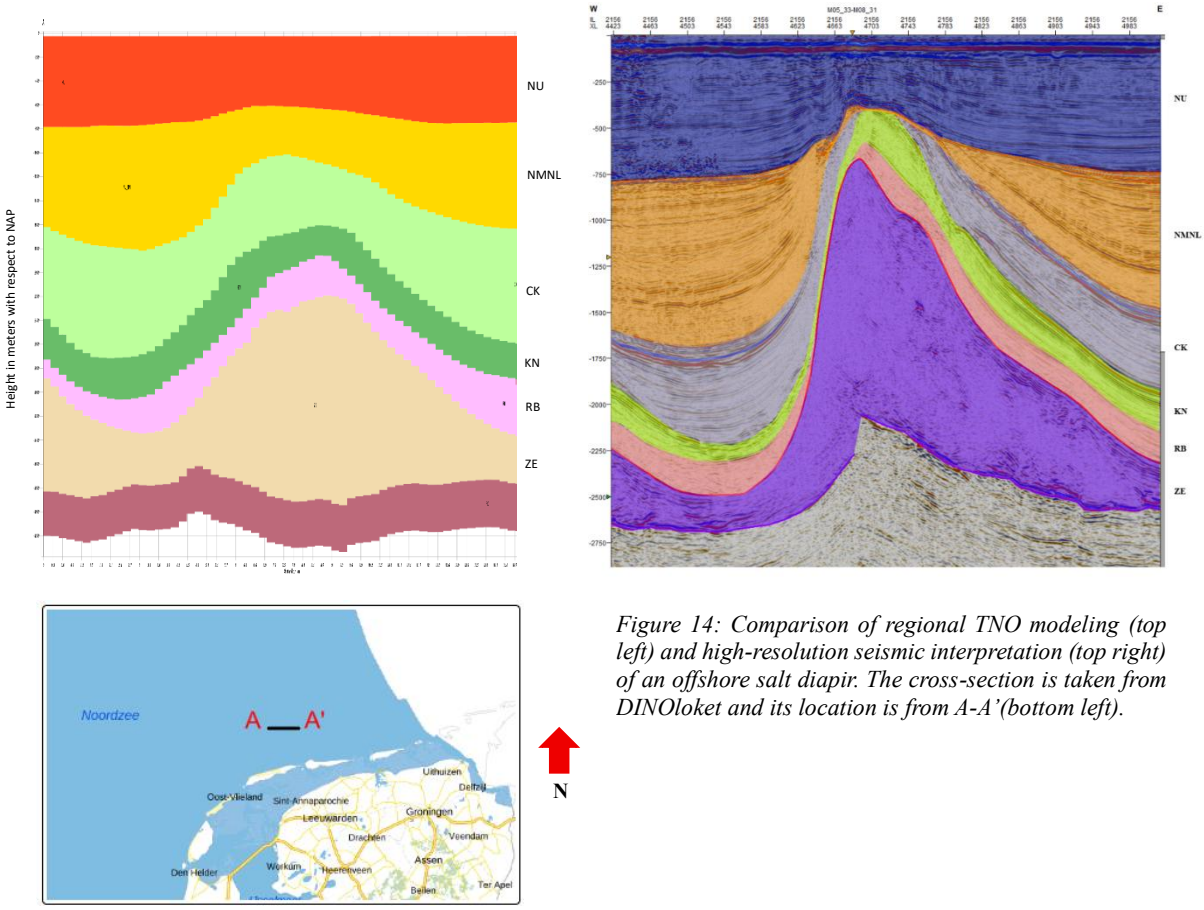

Figure 14: Comparison of regional TNO modeling (top left) and high-resolution seismic interpretation (top right) of an offshore salt diapir. The cross-section is taken from DINOloket and its location is from A-A'(bottom left).

5. Discussion

5.1 Integrating seismic interpretation with the evolution of the salt diapirs: M05-2, M08 and Pieterburen

Offshore: M05-2 and M08

The Ameland Platform is a Mesozoic structural high that flanks the active Terschelling Basin and the Dutch Central Graben. The salt diapirs within blocks M05 and M08 are products of this high-strain environment, where salt served as a detachment layer for massive lateral translation (Bouroullec et al., 2018). The stratigraphic data from the seismic interpretation identifies a discrepancy between the onshore and offshore salt structures regarding the preservation of the RN group. In the onshore Pieterburen diapir, the RN group is present and exhibits truncation and rotation along the salt flanks. Conversely, in the offshore locations M05-2 and M08, the RN group is absent, resulting in the KN group being directly on top of the RB group. The disappearance of the RN group in the offshore areas is attributed to the Hardegsen Unconformity, a regional erosional boundary caused by tectonic tilting and sea-level fluctuations during the Middle Triassic. The Hardegsen phase of extensional tectonics triggered the mobilization of salt and created structural highs (Geluk, 2005). During this phase, vertical salt movement elevated the Triassic overburden, making it susceptible to erosion. This tectonic uplift resulted in the complete removal of the RN group before the deposition of younger Cretaceous sediments in the offshore area. The preservation of the RN group onshore suggests that the Pieterburen region was situated in a rim syncline or experienced less intense erosion during this distinct tectonic phase compared to the offshore platforms (Filomena & Stollhofen, 2011).

The salt diapir from M05-2 seems to be more symmetrical compared to the asymmetric salt diapir in M08. The units RB and KN seem to appear relatively symmetrical on both flanks of the salt diapir when compared to M08. The RB and KN units are thick and continuous on the east flank of the salt diapir where the rim syncline is situated. While on the west flank of the salt diapir the RB and KN are significantly thinned or even absent towards the salt diapir wall. The asymmetry of the salt diapir in M08 is driven by unilateral salt withdrawal (Koyi et al., 2012). Heavy sedimentation on the eastern flank created a differential load that forced Zechstein salt to migrate westward (Warsitzka et al., 2013). This created a rim syncline on the east, providing high accommodation space for the thick continuous RB and KN sequence and a very thin sequence on the west. Conversely, the RB and KN units from the M05-2 salt diapir are relatively symmetrical on both sides. This suggests a more balanced tectonic environment with a more passive growth (Remmelts, 1996).

While both diapirs were impacted by the Late Cretaceous inversion, their stratigraphic expressions differ slightly. M08 exhibits a total crestal unconformity where the CK unit is absent, indicating high-intensity uplift and erosion. In contrast, M05-2 preserves an extremely thin CK sequence over the salt crest. This was subjected to the Alpine inversion during the Late Cretaceous and Early Tertiary (Voet et al., 2019), which is consistent with the characteristics of vertical passive growth for M05-2 versus the active, loading driven migration of M08.

The Cenozoic development of the M05-2 and M08 diapirs aligns with the broader tectonostratigraphic framework of the Dutch North Sea, transitioning from a phase of high-intensity halokinesis in the Paleogene to terminal structural quiescence and burial by the Neogene (Grunnaleite & Mosbron, 2019). This evolution is recorded within the Middle and Lower North Sea Groups (NMNL), which exhibit pronounced stratigraphic thinning toward the diapiric crests. This architecture indicates that during the Paleogene, the rate of salt ascent exceeded the rate of sediment accumulation, maintaining the diapir heads as bathymetric highs that facilitated sediment bypass and the formation of the thinned sections (Bouroullec et al., 2018).

By the Neogene, the deposition of the NU group marked a shift toward regional burial. The relatively uniform thickness of the NU sequence across the crests of both structures signifies that the rate of regional sedimentation overwhelmed the waning rate of salt rise. This phase indicates the exhaustion of the Zechstein salt supply from the source layer, effectively halting the diapirs beneath a post-kinematic sedimentary drape (de Jager et al., 2025; Duin et al., 2006).

Onshore: Pieterburen

Pieterburen is categorized as a mature piercement diapir that has almost reached the current surface, though it remains buried beneath a thin layer of Cenozoic and Quaternary sediments (Back et al., 2022). The Zechstein salt shoulder on the east side of the diapir. This inflection point act as areas of high stress concentrations, which triggered the formation of the extensional faults right above the shoulders that cross cut through the RN, KN and CK unit (Rowan & Krzywiec, 2014).

The thicker RN unit on the west side compared to the east reflects differential salt withdrawal and the formation of a primary rim syncline during the early to mid-Triassic (Back et al., 2022). During this extensional phase, salt migrated away from the Groningen Platform toward depocenters, creating extra accommodation space for the thicker RN accumulation seen on the western flank. The thinning of the RN unit as it approaches the salt crest confirms the structure was already a topographic high during deposition. The thick CK unit and its subsequent thinning at the crest mark the transition from passive to active piercement. This occurred during the Late Cretaceous Subhercynian inversion (Bouroullec et al., 2025), causing it to pierce through the RB, RN, and KN units. The growth strata in the CK unit indicate that the salt rise rate, estimated at 0.01 to 0.02mm/ year (Lauwerier, 2022), exceeded the rate of chalk deposition. The thinning of the NM and NL units indicates continued but slowing diapiric growth during the Paleogene and Neogene, with rates dropping to 0.005 to 0.008mm/year (Lauwerier, 2022). The NU unit draping over the structure records the final burial phase. This unit shows that active piercement had largely ceased where the deposition rate exceeds the salt rise rate. Deposition of the NU unit was accompanied by subrosion (Almalki, 2023; Lauwerier, 2022). This process created a cap rock of insoluble minerals (anhydrite, gypsum, and clay) on top of the Zechstein salt crest (Li et al., 2024).

5.2 The origin and distribution of brittle floaters inside the salt

The internal salt structures identified as floaters in the Pieterburen and offshore diapirs represent primary stratigraphic markers from the Permian Zechstein Group. These features originated from five distinct evaporite cycles (Z1-Z5) where chemical precipitation sequence followed a set order. The five Zechstein salt cycles were deposited during the Late Permian to Early Triassic. Each cycle began with the deposition of carbonates and sulphates such as anhydrite before the formation of halite layers (Geluk, 2010). These non-salt lithologies were originally horizontal sheets with higher density and different mechanical properties than the surrounding halite. During the Hardegsen phase (Triassic extensional phase), the salt began to move. While the halite flowed as a fluid, the stiff carbonate and anhydrite layers could not deform plastically. These brittle layers were stretched until they ruptured into fragments. These fragments then became “floaters” that were carried upwards by the rising salt rock.

5.3 Long term disposal analyses and its integrity

Results indicate more heterogeneity in Pieterburen and M08 in comparison with M05-1. Floaters occur at the base and flanks of these diapirs in frequencies that surpass M05-1. In the interval above 1200 meters depth, impurities in Pieterburen and M08 exist in proportions that still exceed M05-1. Pieterburen has the thickest caprock while M05-1 has the thinnest caprock among these salt diapirs.

Rock salt provides a combination of impermeability and self-sealing capacity that makes it a favourable host rock for waste isolation. The presence of non-salt lithologies such as anhydrite and carbonate floaters introduces heterogeneity in mechanical strength, permeability, and dissolution potential. These brittle internal structures do not flow or self-heal like halite and can act as pathways for fluid migration or create mechanical weaknesses within the rock mass. Rock heterogeneity and fractures cause abrupt spatial changes in capillary action and flow characteristics, leading to uneven distributions of subsurface interactions (He et al., 2023). Intra-salt intercalations influence the mechanical behaviour of diapirs and are a key factor in reducing predictability for geological models (Auzemery et al., 2025). While a thick caprock can function as a secondary barrier to fluid flow, its thickness and composition are indicators of the intensity and duration of past subrosion processes. M08 and Pieterburen shows that thick caprocks are often associated with chaotic seismic character and crestal sags, which indicate active dissolution and potential instability of the natural barrier. In addition, the caprock data is in alignment with Auzemary (2025), demonstrating that the caprock exhibits increased thickness in areas where the salt diapir is situated at shallower subsurface depths. Conversely, a systematic thinning of the caprock is observed as the diapiric crest lies deeper in the stratigraphic levels.

This report also evaluated the layout for the high and low waste facilities of COVRA (Bartol, 2024), where the design uses levels to reduce the footprint. The disposal fits withing the three diapirs that were studied in this report (see appendix for the measurements). The facility remains within the boundaries of the structures since the configuration allows the repository to stay within the formation of salt.

5.4 Limitations

A limitation in the onshore Pieterburen area was the distribution of available well data relative to the salt diapir structure. While numerous wells were drilled in the vicinity of the diapir, only one borehole, PBN-01, directly intersected the top of the salt body. All other available wells were situated either around the flanks or in close proximity, but did not penetrate the salt diapir itself. This configuration restricted the ability to perform definitive well-tie correlations directly at the salt interface. Because the lack of wells going through the salt diapir body there is an uncertainty in delineating the precise salt margins and the geometry of adjacent stratigraphic layers, particularly near the steeply dipping flanks of the salt diapir.

The interpretation of the onshore seismic survey was also affected by a data quality issue observed in the shallowest unit, the Upper North Sea (NU) layer. The seismic reflectors within this interval exhibit a distinct wavy artifact. This phenomenon is typically caused by multiple reverberation or rebounce of seismic energy trapped between two strong acoustic impedance boundaries, such as the seabed and a hard, shallow layer, or between two strong shallow reflectors themselves. The effect is a rapid sequence of spurious, low-amplitude reflectors that mimic the primary reflection pattern, thereby obscuring the true geological dip and structure of the NU layer and increasing the ambiguity of its interpretation (Fig. 15). Despite the presence of the wavy artifact, which complicated the precise interpretation of the reflectors within the Upper North Sea (NU) layer, the main line trend of the stratigraphic horizon could still be approximately followed and delineated.

Furthermore, the offshore study area data was limited due to a pronounced scarcity of borehole data. Compared to the onshore area, only a handful of wells were available, and these were only in the immediate vicinity of the offshore salt diapirs. None of these boreholes penetrated the offshore salt diapirs themselves. This complete lack of direct penetration meant that less continuous reliable well-tie connections could be established, resulting in a slightly higher degree of uncertainty in the interpreted structural geometry for the offshore area.

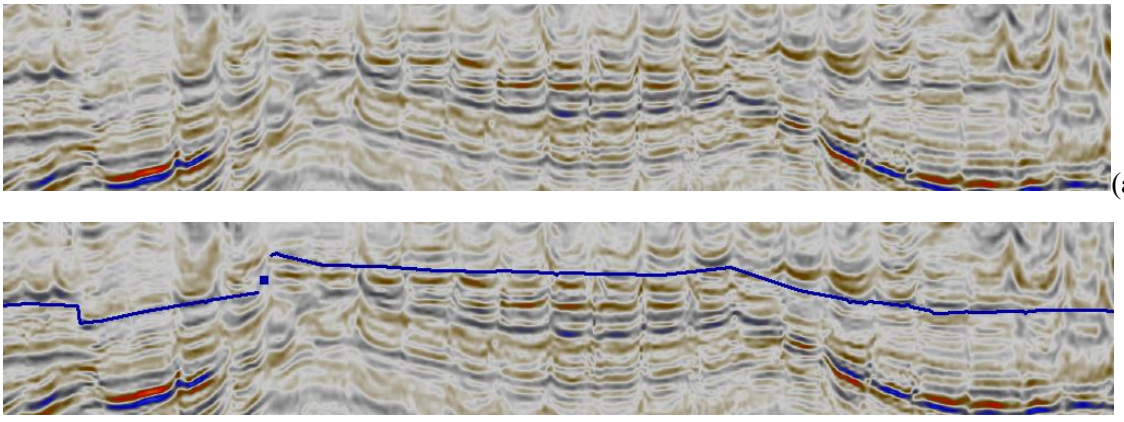

Figure 15 (a-b): Figure (a) shows the wavy artifact in the upper stratigraphy, and figure (b) shows the Upper North Sea (NU) line trace.

Lastly, direct comparison between the studied diapirs and DINOloket models was limited by discrepancies in coordinate systems, which prevented the extraction of identical cross-sections from Petrel. Consequently, precise correlations of salt crest depths and thicknesses could not be established.

For example, this study identifies the Pieterburen crest at a depth of 180–200 m, whereas the DINOloket model indicates a depth of 600m (Fig. 7). However, a TNO research paper (TNO, 2014) reports the Pieterburen crest depth at approximately 220 m, which aligns more closely with the findings of this study. These variances demonstrate that a feasible comparison requires the use of identical cross-sectional data across both platforms.

6. Conclusion

Summarized, the investigation into the Pieterburen, M05-2, and M08 salt structures reveals a complex history of halokinesis initiated by Late Permian evaporite deposition across five primary cycles (Z1-Z5). Structural mapping identifies Pieterburen as a mature, high-relief diapir that has almost reached the surface, currently buried under a thin layer of Cenozoic and Quaternary sediments. Offshore, the M05-2 and M08 diapirs are mature piercement structures that exhibit significant upward drag of adjacent sedimentary layers. M05-1 is identified as having higher halite purity, while the Pieterburen and M08 structures contain brittle anhydrite and carbonate floaters that increase mechanical heterogeneity. Furthermore, caprock thickness correlates with crestal depth, with the shallowest structures exhibiting the most extensive dissolution residue.

The evolution of these diapirs began with Mid-Triassic mobilization triggered by the Hardegsen phase of extensional tectonics. During this period, the brittle carbonate and anhydrite sheets within the halite ruptured into the fragments now identified as floaters. In offshore blocks M05 and M08, this tectonic phase resulted in the Hardegsen Unconformity and the complete removal of the RN stratigraphic group. In contrast, the Pieterburen region was situated in a rim syncline, preserving the RN group despite subsequent truncation. Jurassic rifting further remobilized the salt into large diapiric structures, creating rim synclines that accommodated thick sequences of syn-rift sediments. The Late Cretaceous Subhercynian inversion accelerated this growth, forcing the salt to pierce the Triassic and Cretaceous overburden. At Pieterburen, the salt rose faster than chalk deposition, resulting in the thinning and rotation of the Chalk Group. Offshore M08 experienced asymmetric growth due to differential sedimentary loading on its eastern flank, forcing salt migration toward a western structural wall.

In conclusion, The refined 3D models demonstrate that while halokinesis persisted into the Cenozoic, the structures have transitioned from active piercement to a diminishing stage of draped growth. The uniform thickness of the Neogene Upper North Sea group indicates that regional sedimentation has overwhelmed the waning salt supply, effectively burying the diapirs beneath a post-kinematic drape. Despite the presence of internal impurities and the risks of active subrosion, the studied salt structures provide adequate spatial boundaries to accommodate current repository configurations for radioactive waste isolation.

7. References

Alexandre, J. P. T., & Wong, T. E. (2025). Rhaetian to Middle Jurassic. In *Geology of the Netherlands* (2nd edn). Routledge.

Almalki, B. (2023). *Zechstein Salt Structures Evolution in the Northeastern Netherlands*.

Auzemery, A., Matenco, L., & Nader, F. (2025). Understanding the distribution of lithologies in Zechstein salt diapirs and their impact on quantifying subrosion in the Netherlands for the safety of nuclear waste disposal repositories. *2025*.

Back, S., Amberg, S., Sachse, V., & Littke, R. (2022). *Reconstructing 3D subsurface salt flow*. Crustal structure and composition/Stratigraphy, sedimentology, geomorphology, morphotectonics, and palaeontology/Stratigraphy. https://doi.org/10.5194/se-2021-153

Bartol, J. (2024). Copera Salt 2024. *2024*.

Bérest, P., Gharbi, H., Blanco-Martín, L., Brouard, B., Brückner, D., DeVries, K. L., Hévin, G., Hofer, G., Spiers, C. J., & Urai, J. L. (2023). Salt Creep: Transition Between the Low and High Stress Domains. *Rock Mechanics and Rock Engineering*, *56*(11), 8305–8316. https://doi.org/10.1007/s00603-023-03485-y

Bouroullec, R., Geel, C. R., & Geluk, M. C. (2025). Permian. In *Geology of the Netherlands* (2nd edn). Routledge.

Bouroullec, R., Verreussel, R. M. C. H., Geel, C. R., de Bruin, G., Zijp, M. H. A. A., Kőrösi, D., Munsterman, D. K., Janssen, N. M. M., & Kerstholt-Boegehold, S. J. (2018). Tectonostratigraphy of a rift basin affected by salt tectonics: Synrift Middle Jurassic–Lower Cretaceous Dutch Central Graben, Terschelling Basin and neighbouring platforms, Dutch offshore. *Geological Society, London, Special Publications*, *469*(1), 269–303. https://doi.org/10.1144/SP469.22

Cosenza, Ph., Ghoreychi, M., Bazargan-Sabet, B., & de Marsily, G. (1999). In situ rock salt permeability measurement for long term safety assessment of storage. *International Journal of Rock Mechanics and Mining Sciences*, *36*(4), 509–526. https://doi.org/10.1016/S0148-9062(99)00017-0

De Jager, J. (2003). Inverted basins in the Netherlands, similarities and differences. *Netherlands Journal of Geosciences - Geologie En Mijnbouw*, *82*(4), 339–349. https://doi.org/10.1017/S0016774600020175

de Jager, J., van Ojik, K., & Smit, J. (2025). *Geological development* (pp. 21–51). https://doi.org/10.2307/jj.27435714.5

Doornenbal, J. C. (2020). *Velmod-4*.

Duin, E. J. T., Doornenbal, J. C., Rijkers, R. H., Verbeek, J. W., & Wong, T. E. (2006). Subsurface structure of the Netherlands-results of recent onshore and offshore mapping. *Netherlands Journal of Geosciences*, *85*(4), 245.

Filomena, C. M., & Stollhofen, H. (2011). Ultrasonic logging across unconformities—Outcrop and core logger sonic patterns of the Early Triassic Middle Buntsandstein Hardegsen unconformity, southern Germany. *Sedimentary Geology*, *236*(3), 185–196. https://doi.org/10.1016/j.sedgeo.2011.01.005

Gee, D. G., Janák, M., Majka, J., Robinson, P., & van Roermund, H. (2013). Subduction along and within the Baltoscandian margin during closing of the Iapetus Ocean and Baltica-Laurentia collision. *Lithosphere*, *5*(2), 169–178. https://doi.org/10.1130/L220.1

Geluk, M. (1999). Late Permian (Zechstein) rifting in the Netherlands; models and implications for petroleum geology. *Petroleum Geoscience*, *5*(2), 189–199. https://doi.org/10.1144/petgeo.5.2.189

Geluk, M. (2010). Zoutmeren en –zeeën in de Nederlandse ondergrond. *Grondboor & Hamer*, *64*(4/5), 103–110.

Geluk, M. C. (2005, February 24). *Stratigraphy and tectonics of Permo-Triassic basins in the Netherlands and surrounding areas* [Dissertation]. Utrecht University. https://dspace.library.uu.nl/handle/1874/1699

Geluk, M. C., & Röhling, H.-G. (1997). High-resolution sequence stratigraphy of the Lower Triassic 'Buntsandstein' in the Netherlands and northwestern Germany. *Geologie En Mijnbouw*, *76*(3), 227–246. https://doi.org/10.1023/A:1003062521373

Grunnaleite, I., & Mosbron, A. (2019). On the Significance of Salt Modelling—Example from Modelling of Salt Tectonics, Temperature and Maturity Around Salt Structures in Southern North Sea. *Geosciences*, *9*(9), 363. https://doi.org/10.3390/geosciences9090363

Harding, R., & Huuse, M. (2015). Salt on the move: Multi stage evolution of salt diapirs in the Netherlands North Sea. *Marine and Petroleum Geology*, *61*, 39–55. https://doi.org/10.1016/j.marpetgeo.2014.12.003

He, D., Jiang, P., & Xu, R. (2023). The influence of heterogeneous structure on salt precipitation during CO2 geological storage. *Advances in Geo-Energy Research*, *7*(3), 189–198. https://doi.org/10.46690/ager.2023.03.05

Houben, M. E., ten Hove, A., Peach, C. J., & Spiers, C. J. (2013). Crack healing in rocksalt via diffusion in adsorbed aqueous films: Microphysical modelling versus experiments. *Physics and Chemistry of the Earth, Parts A/B/C, Coupled Physical and Chemical Transformations Affecting the Performance of GeoSystems*, *64*, 95–104. https://doi.org/10.1016/j.pce.2012.10.001

Huuse, M., & Clausen, O. R. (2001). Morphology and origin of major Cenozoic sequence boundaries in the eastern North Sea Basin: Top Eocene, near-top Oligocene and the mid-Miocene unconformity. *Basin Research*, *13*(1), 17–41. https://doi.org/10.1046/j.1365-2117.2001.00123.x

Jager, J. D. (2012). The discovery of the Fat Sand Play (Solling Formation, Triassic), Northern Dutch offshore – a case of serendipity. *Netherlands Journal of Geosciences - Geologie En Mijnbouw*, *91*(4), 609–619. https://doi.org/10.1017/S0016774600000408

Karlo, J. F., van Buchem, F. S. P., Moen, J., & Milroy, K. (2014). Triassic-age salt tectonics of the Central North Sea. *Interpretation*, *2*(4), SM19–SM28. https://doi.org/10.1190/INT-2014-0032.1

Koyi, H., Burliga, S., & Chemia, Z. (2012). *Salt supply to and significance of asymmetric salt diapirs*. 10365. https://ui.adsabs.harvard.edu/abs/2012EGUGA..1410365K

Lauwerier, W. (2022). *E VOLUTION OF THE ZECHSTEIN SALT DIAPIRS IN THE NORTH EASTERN NETHERLANDS.*

Li, M., Collard, N., Schueller, S., Matenco, L., Nader, F. H., Beekman, F., Cacas, M.-C., & Bartol, J. (2024). *Quantitative modelling of diapirism and geochemical evolution of the subrosion process of salt domes in the northeast Netherlands for radioactive waste disposal*.

Maystrenko, Y. P., Bayer, U., & Scheck-Wenderoth, M. (2013). Salt as a 3D element in structural modeling—Example from the Central European Basin System. *Tectonophysics, Basin Dynamics*, *591*, 62–82. https://doi.org/10.1016/j.tecto.2012.06.030

PENGE, J., MUNNS, J. W., TAYLOR, B., & WINDLE, T. M. F. (1999). Rift–raft tectonics: Examples of gravitational tectonics from the Zechstein basins of northwest Europe. *Geological Society, London, Petroleum Geology Conference Series*, *5*(1), 201–213. https://doi.org/10.1144/0050201

Pichat, A. (2022). Stratigraphy, Paleogeography and Depositional Setting of the K–Mg Salts in the Zechstein Group of Netherlands—Implications for the Development of Salt Caverns. *Minerals*, *12*(4), 486. https://doi.org/10.3390/min12040486

Remmelts, G. (1996). Salt tectonics in the southern North Sea, the Netherlands. In H. E. Rondeel, D. A. J. Batjes, & W. H. Nieuwenhuijs (Eds), *Geology of Gas and Oil under the Netherlands: Selection of papers presented at the 1983 Iternational Conference of the American Association of Petroleum Geologists, held in The Hague* (pp. 143–158). Springer Netherlands. https://doi.org/10.1007/978-94-009-0121-6_13

Remmelts, G. (2011). *Mogelijke alternatieven voor ondergrondse opslag van gas in de zoutkoepel Pieterburen.*

Roel, M. C. H. V. (2025). *Late Jurassic – Early Cretaceous*.

Rowan, M. G., & Krzywiec, P. (2014). The Szamotuły salt diapir and Mid-Polish Trough: Decoupling during both Triassic-Jurassic rifting and Alpine inversion. *Interpretation*, *2*(4), SM1–SM18. https://doi.org/10.1190/INT-2014-0028.1

TNO. (2014). *Zoutkoepel pieterburen*. https://www.google.com/search?q=zoutkoepel+pieterburen&rlz=1C1YTUH_nlNL1037NL1037&oq=zoutkoepel+pieterburen&gs_lcrp=EgZjaHJvbWUyCggAEEUYFhgeGDkyCggBEAAYgAQYogQyCggCEAAYgAQYogQyCggDEAAYgAQYogQyBwgEEAAY7wXSAQgyOTY0ajBqN6gCCLACAfEF2ZUHPzi7UDE&sourceid=chrome&ie=UTF-8

Veen, J. H. ten, Gessel, S. F. van, & Dulk, M. den. (2012). Thin- and thick-skinned salt tectonics in the Netherlands; a quantitative approach. *Netherlands Journal of Geosciences*, *91*(4), 447–464. https://doi.org/10.1017/S0016774600000330

Verweij, J. M. (2003). *Fluid flow systems analysis on geological timescales in onshore and offshore Netherlands. With special reference to the Broad Fourteens Basin.* [PhD-Thesis – Research external, graduation internal]. NSG.

Voet, E. V. D., Heijnen, L., & Reijmer, J. J. G. (2019). Geological evolution of the Chalk Group in the northern Dutch North Sea: Inversion, sedimentation and redeposition. *Geological Magazine*, *156*(7), 1265–1284. https://doi.org/10.1017/S0016756818000572

Warsitzka, M., Kley, J., & Kukowski, N. (2013). Salt diapirism driven by differential loading—Some insights from analogue modelling. *Tectonophysics, Basin Dynamics*, *591*, 83–97. https://doi.org/10.1016/j.tecto.2011.11.018

Zeng, Z., Ma, H., Yang, C., Zhao, K., Liang, X., Li, H., & Zheng, Z. (2024). Self-healing behaviors of damaged rock salt under humidity cycling. *International Journal of Rock Mechanics and Mining Sciences*, *174*, 105636. https://doi.org/10.1016/j.ijrmms.2024.105636

Zhang, Y., Krause, M., & Mutti, M. (2013). The Formation and Structure Evolution of Zechstein (Upper Permian) Salt in Northeast German Basin: A Review. *Open Journal of Geology*, *3*(8), 411–426. https://doi.org/10.4236/ojg.2013.38047

8. Appendix

Study area

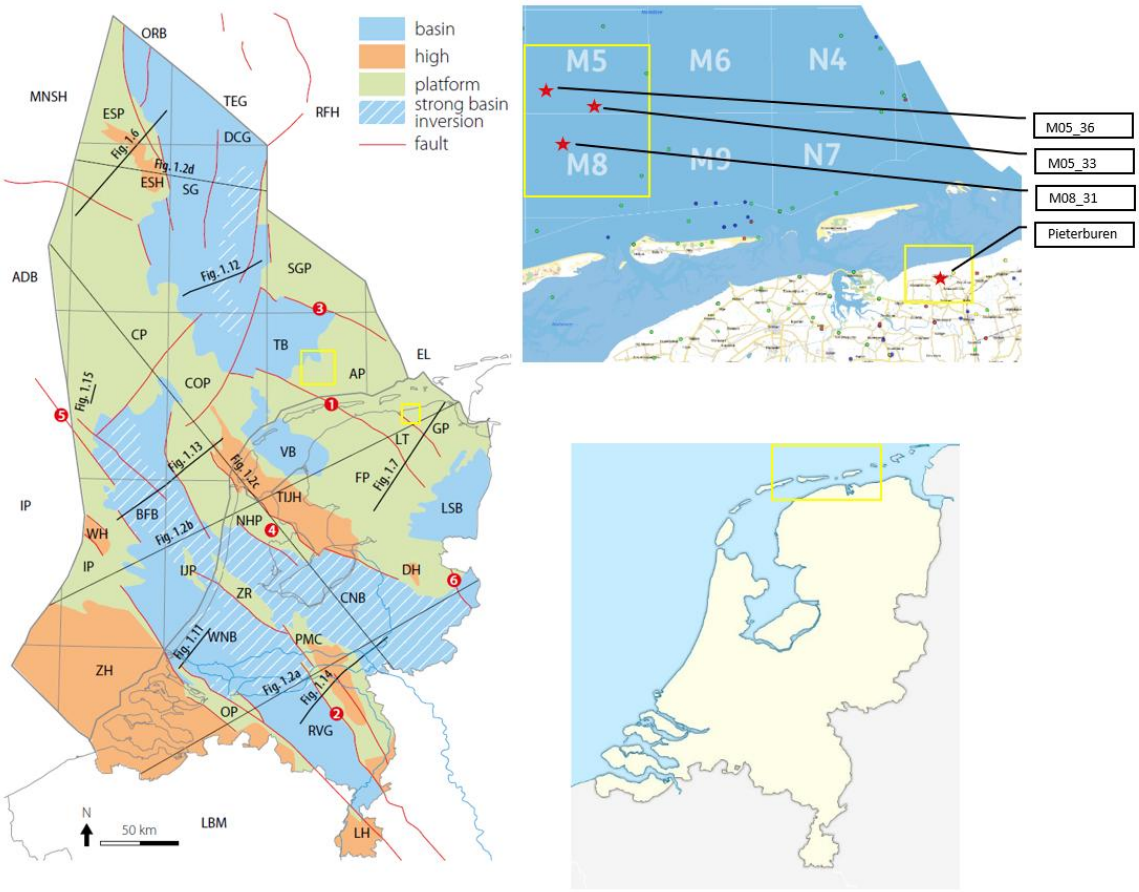

Pieterburen salt diapir

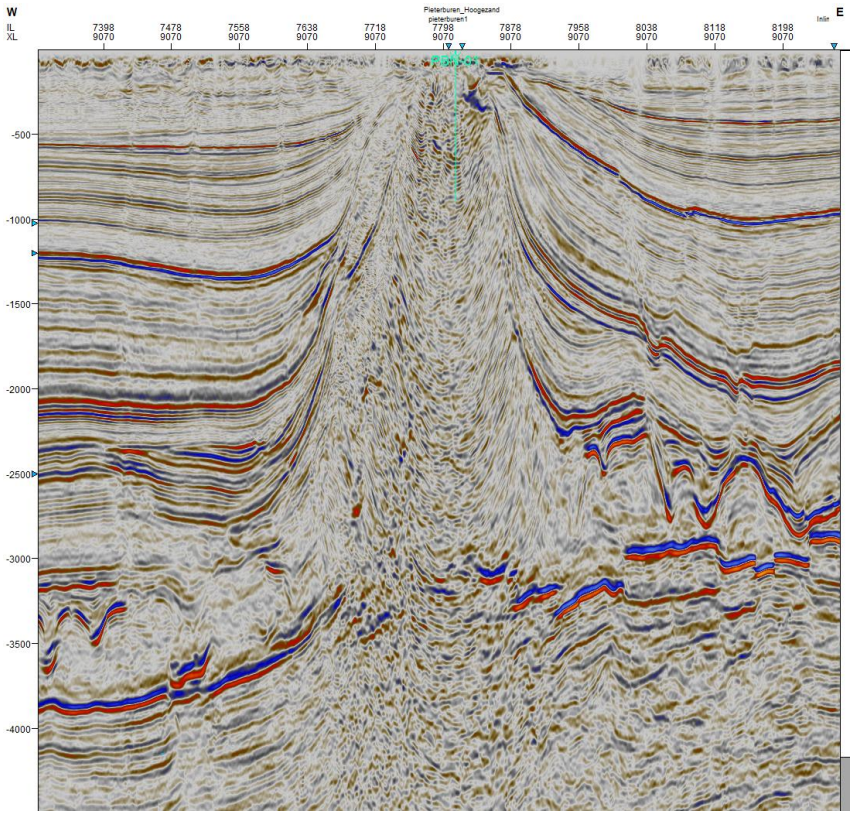

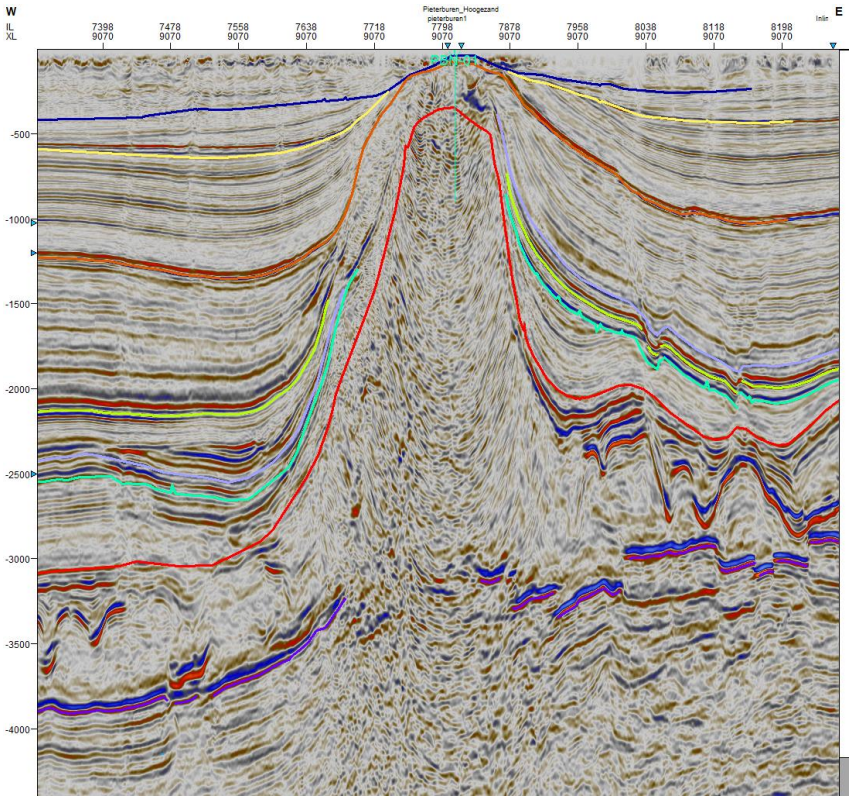

M05-2 salt diapir

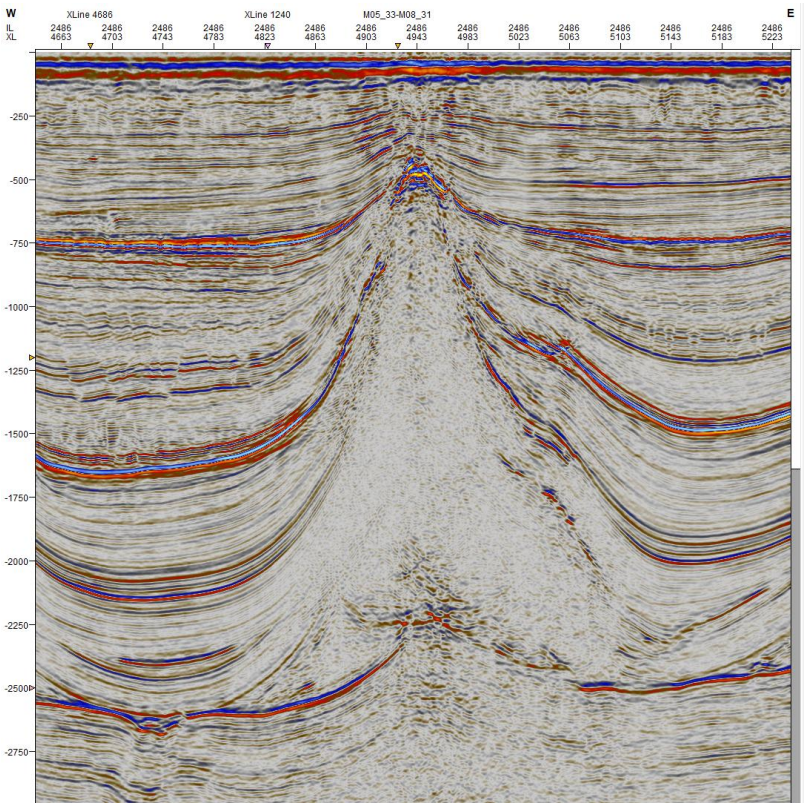

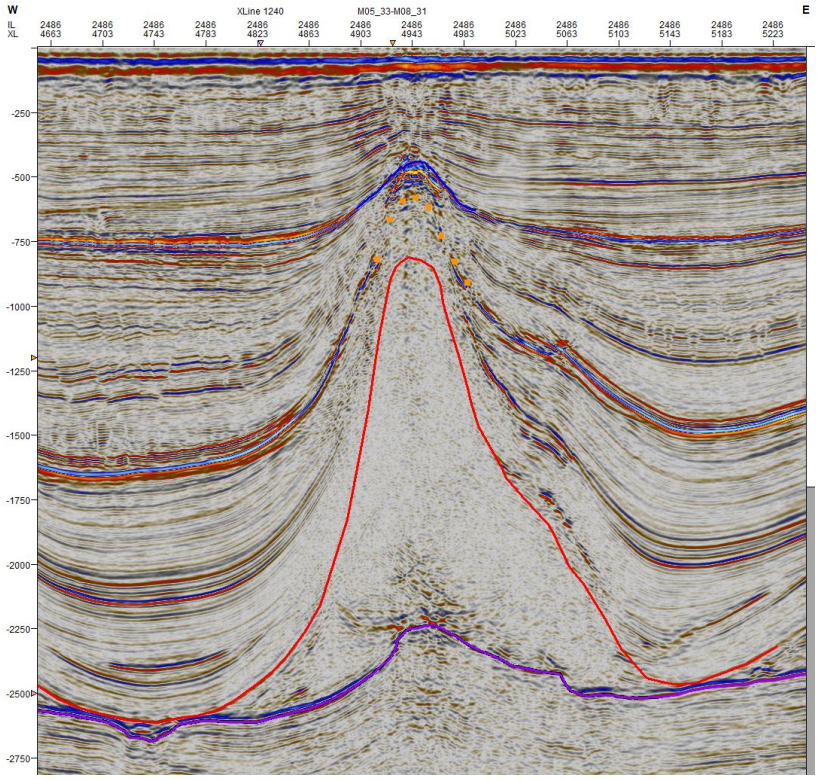

M08 salt diapir

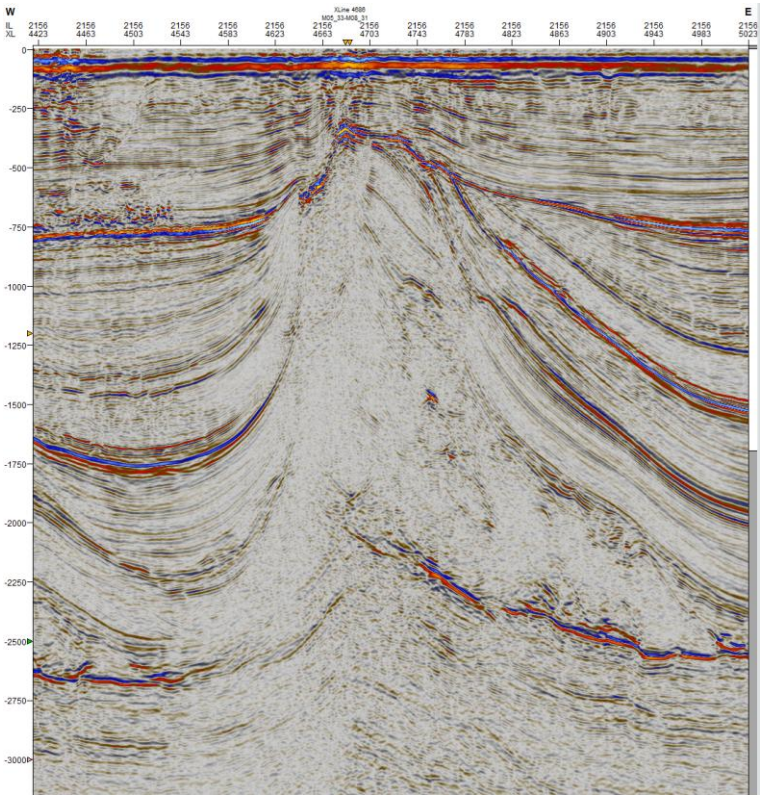

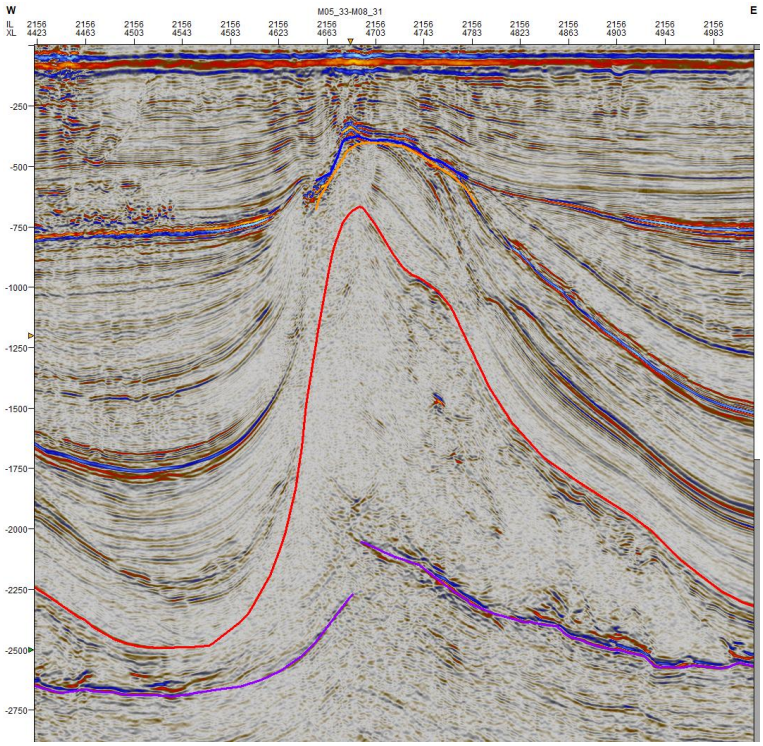

Pieterburen salt diapir top trace with TNO model

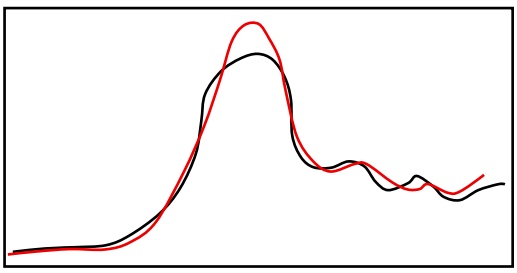

Wells onshore surrounding Pieterburen, only PBN-01 well penetrates the top part of the salt diapir.

well number	3C	3D	6F	7A	7B	7C
Well number information	EEN-OBS	ODP-01	KBB-01	LNS-01	BDM-01	FAN-01
	PBN-01	USQ-01	KBB-01-S1	LNS-01-S1	BDM-02	FAN-02
		USQ-QBS	KBB-01-S2	LNS-02	BDM-03	PSP-01
		WRF-01	KBB-01-S3	RAN-01	BDM-04	PSP-02
		WRF-02	KBB-02-S4	SSM-01	BDM-05	PSP-02-S1
		WRF-02-S1	KBB-02	SSM-01-S1	RDW-01	PSP-02-S2
		WRF-02-S2	KBB-02-S1	SSM-02	SAU-01	PSP-03
			KBB-02-S2	SSM-02-S1	WSM-01	
			KBB-03	SSM-03	WSM-OBS	
			KBB-04	SSM-03-S1		
			KBB-05	SSM-04		
			MKZ-01			
			MKZ-01-S1			
			MKZ-02			
			MKZ-02-S1			
			MKZ-02-S2			
			MKZ-02-S3			
			MKZ-03			
			MKZ-04			
			MKZ-04-S1			
			MKZ-05			
			MKZ-05-0S1			
			MKZ-06			

	MKZ-07
	WFM-01
	WFM-02
	WFM-03
	VHN-01
	VHN-01-S1
	VHN-01-S2
	VHN-01-S3
	VHN-02
	VHN-03
	VHN-03-S1
	GRK-01
	GRK-01-S1
	GRK-02
	GRK-03
	GRK-11
	GRK-13
	GRK-15
	GRK-17
	GRK-17-S1
	GRK-21
	GRK-43
	GRK-45
	GRK-47
	LWZ-01
	LWZ-02
	LWZ-03
	LWZ-03-S1

offshore	Well numbers
	M05-01
	M07-01
	M07-04
	M07-10
	M08-01
	M08-02
	M09-01
	M10-01
	M10-05
	M11-01

Onshore Pieterburen

ZE base surface

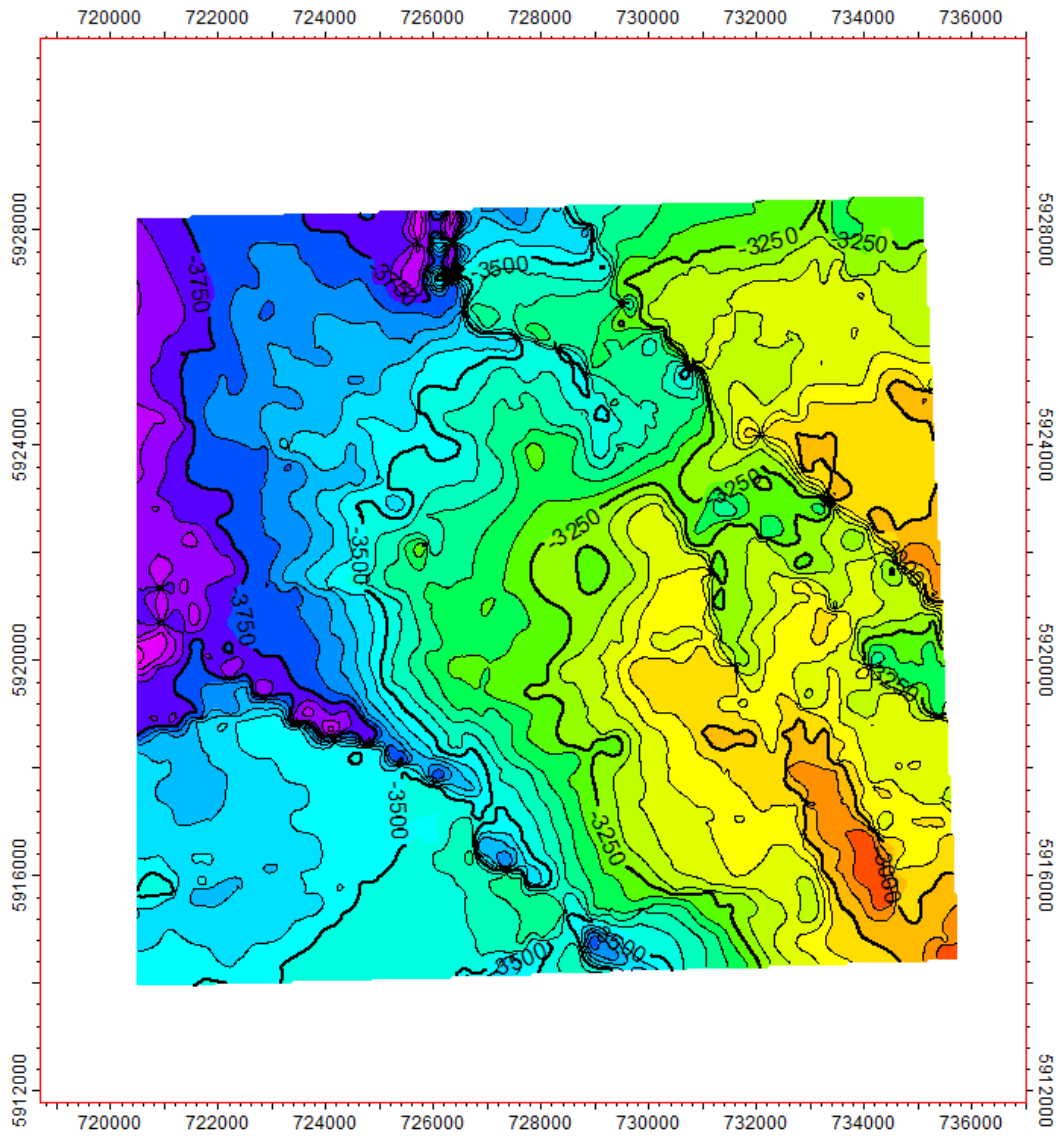

RB base/ ZE top surface

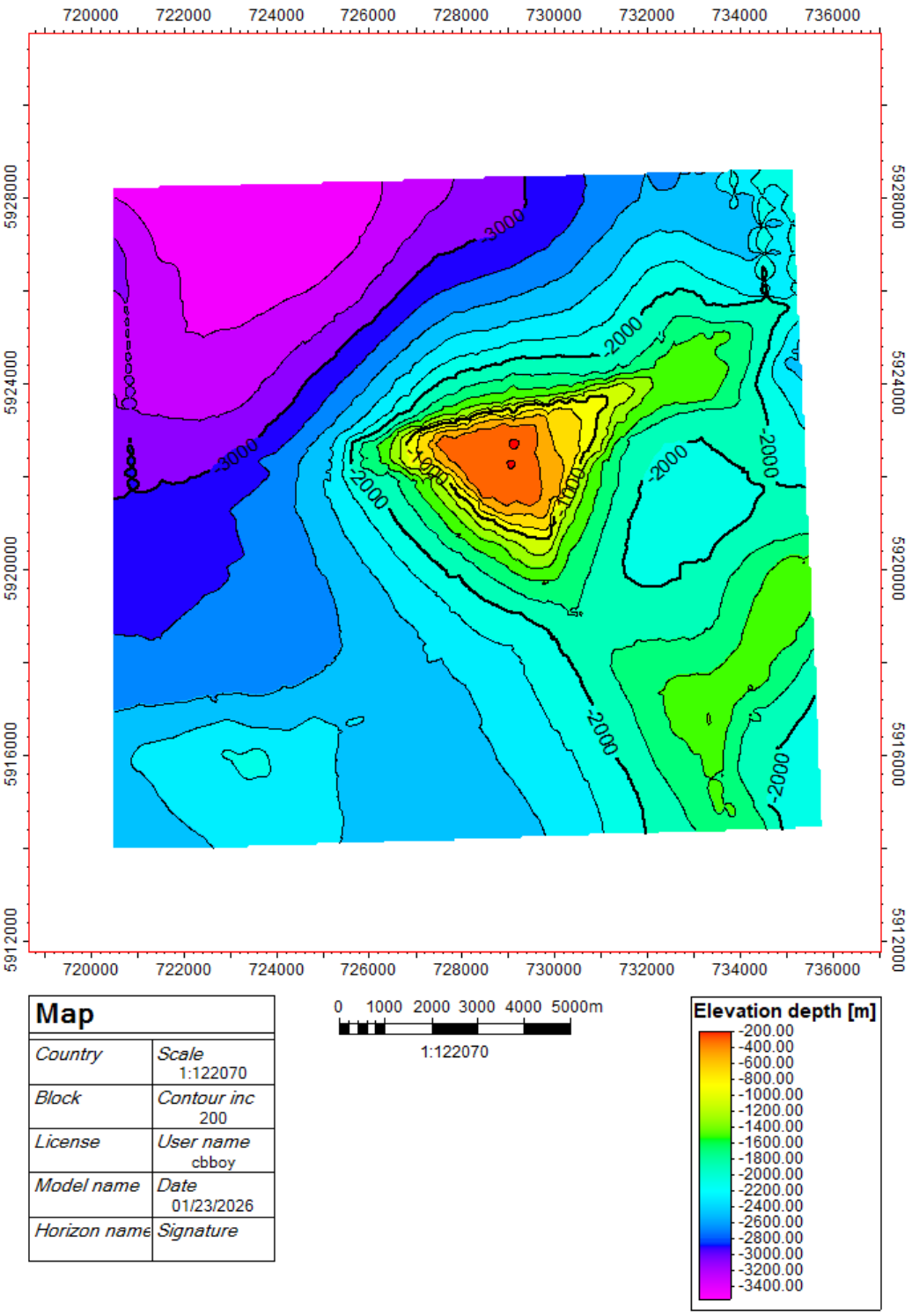

RN base surface, IGNORE TOP PART, BECAUSE TOP IS PIERCED BY SALT DIAPIR

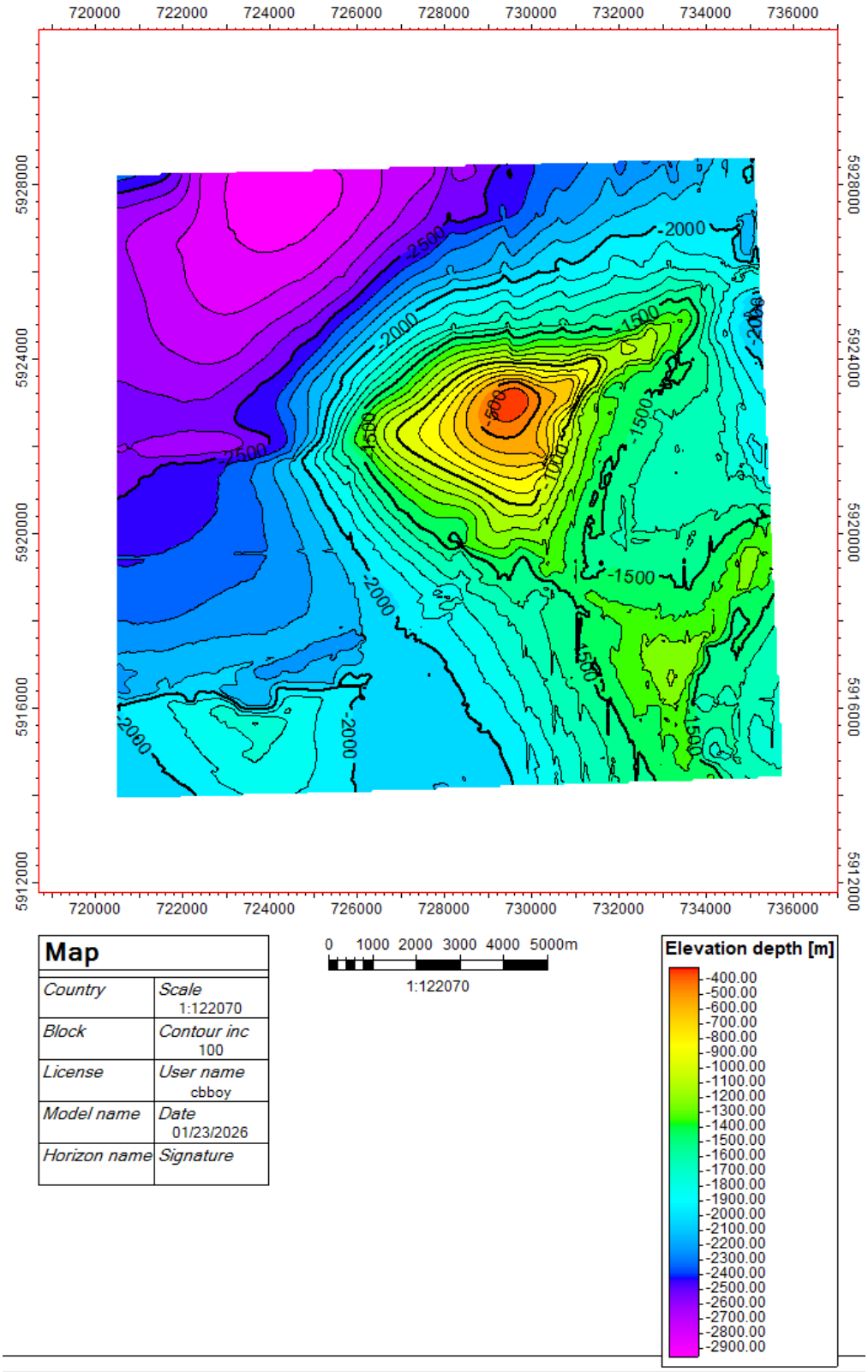

KN base surface, IGNORE TOP PART, BECAUSE TOP IS PIERCED BY SALT DIAPIR

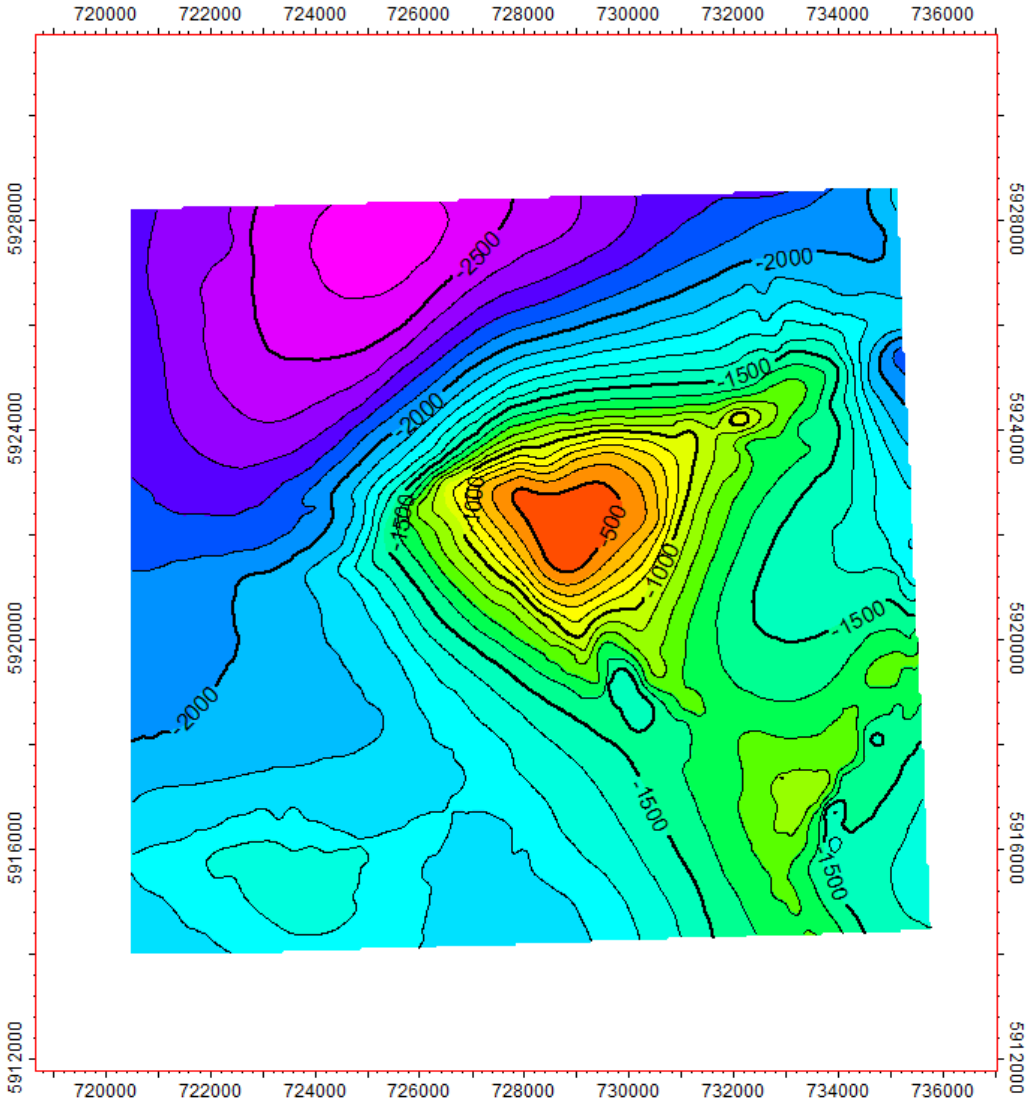

Map	
Country	*Scale* 1:122070
Block	*Contour inc* 100
License	*User name* cbboy
Model name	*Date* 01/23/2026
Horizon name	*Signature*

0 1000 2000 3000 4000 5000m

1:122070

Elevation depth [m]

-500.00
-600.00
-700.00
-800.00
-900.00
-1000.00
-1100.00
-1200.00
-1300.00
-1400.00
-1500.00
-1600.00
-1700.00
-1800.00
-1900.00
-2000.00
-2100.00
-2200.00
-2300.00
-2400.00
-2500.00
-2600.00

NL base surface

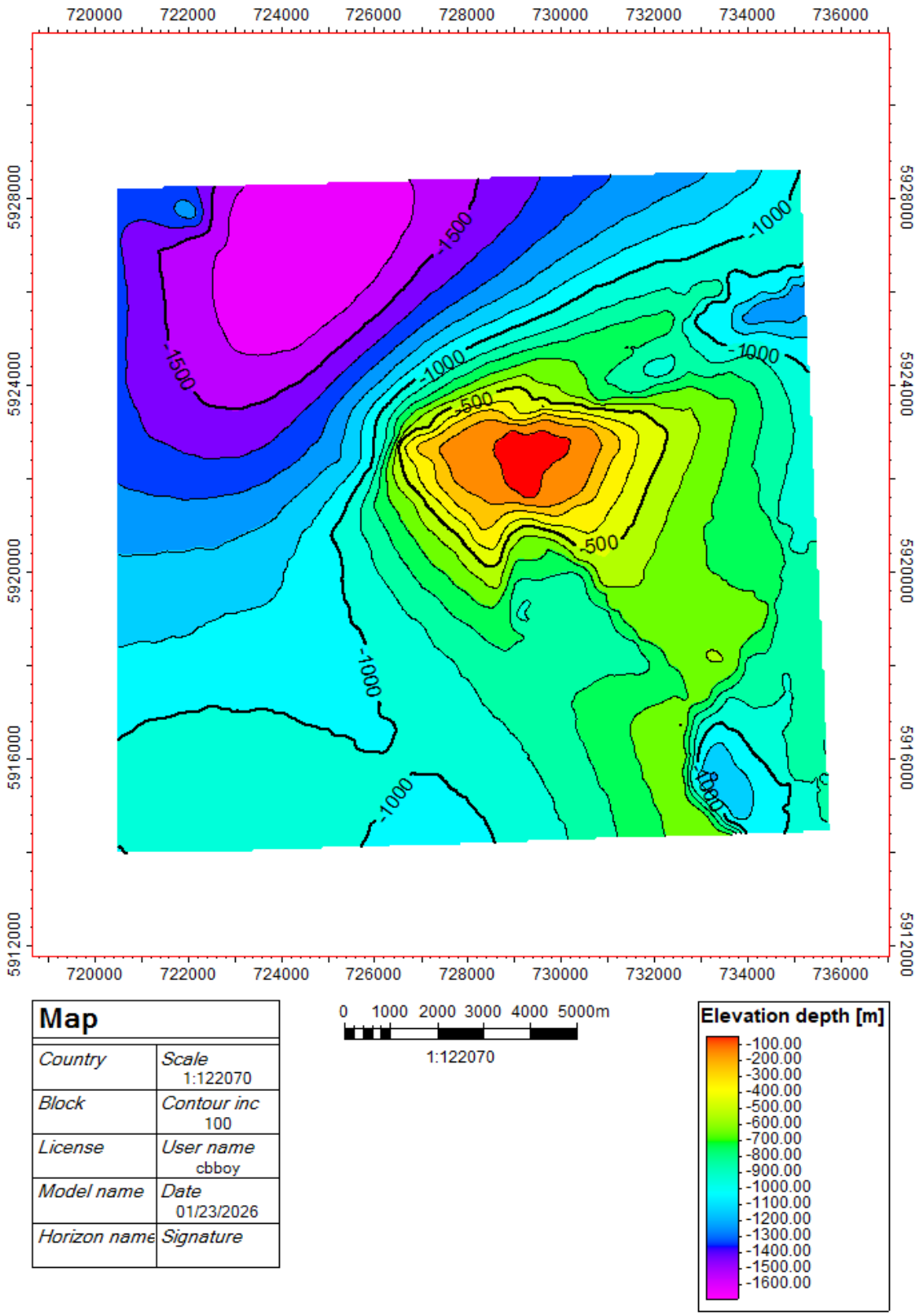

NM base surface

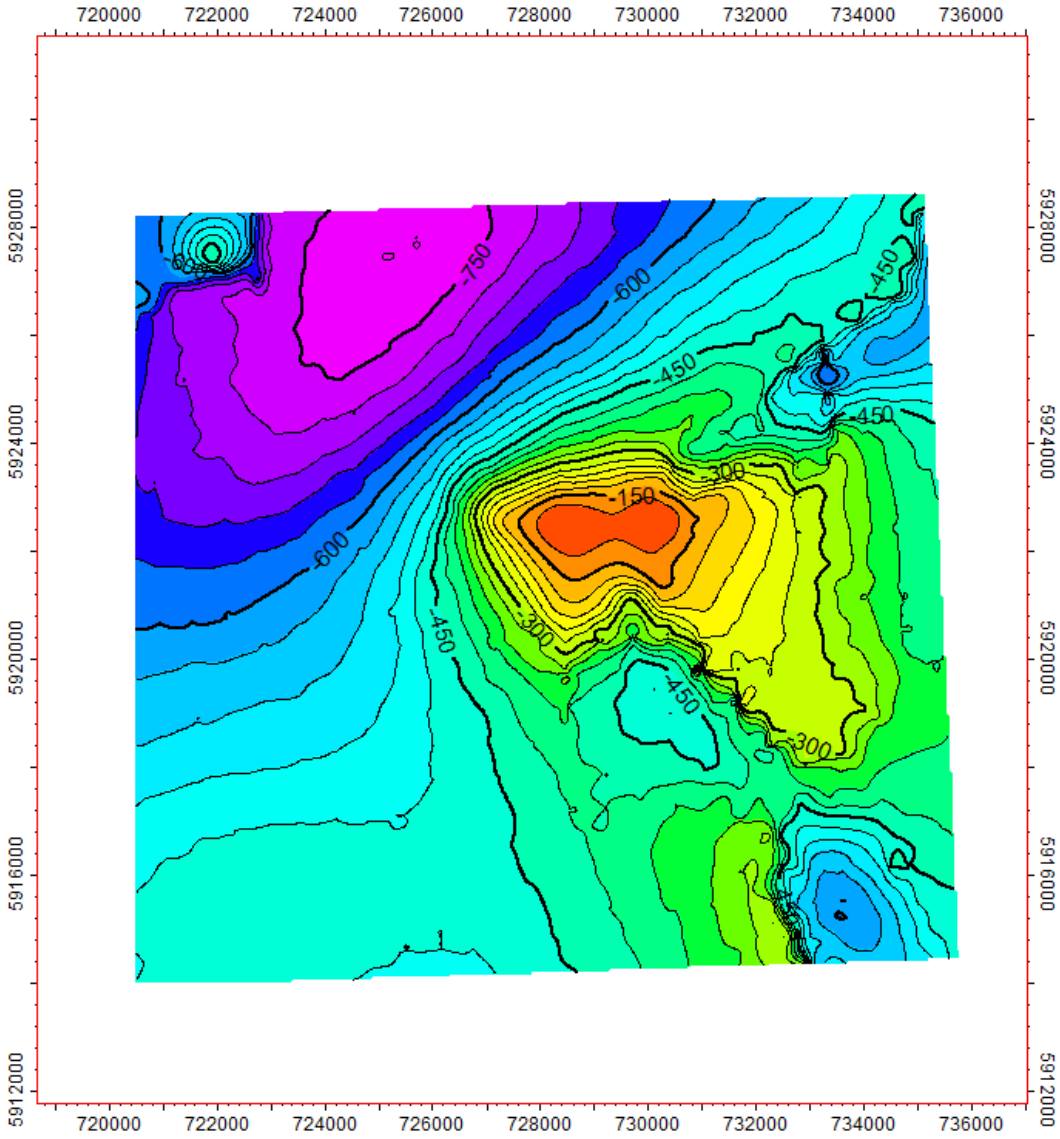

NU base surface, the focus is only inside the red box, seismic lines were only traced inside this red box.

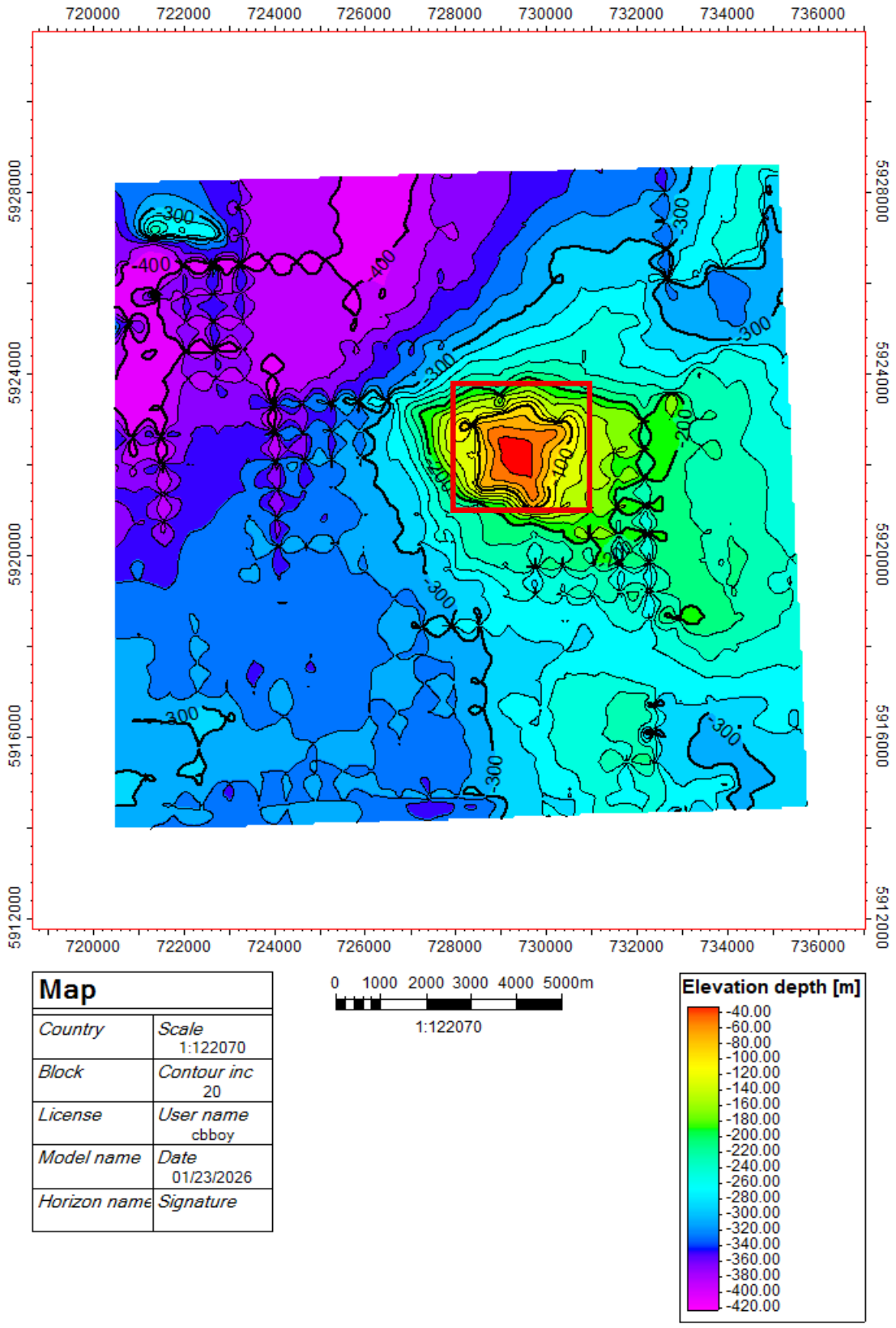

Off-shore

ZE top surface

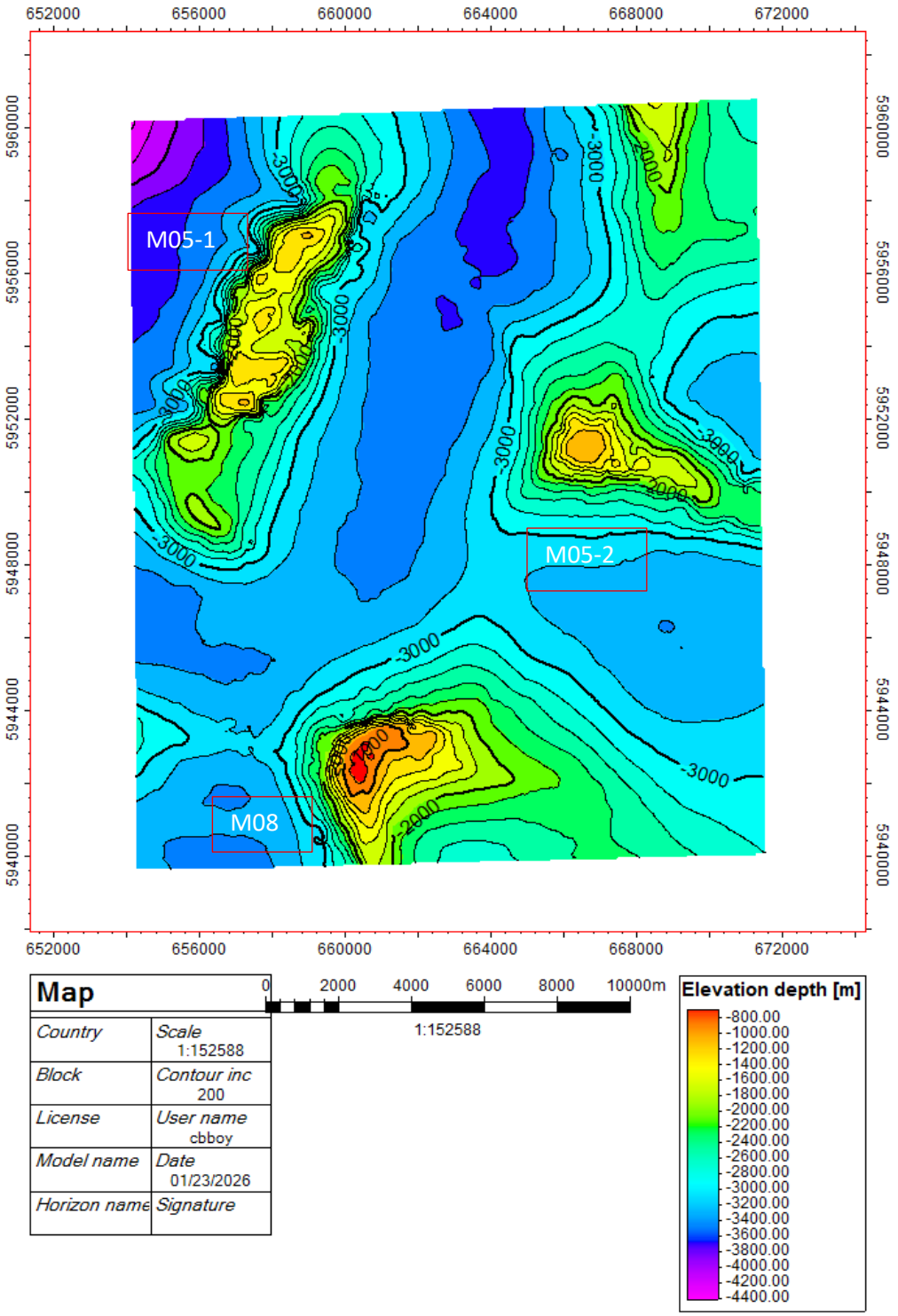

M05-2 NL base surface

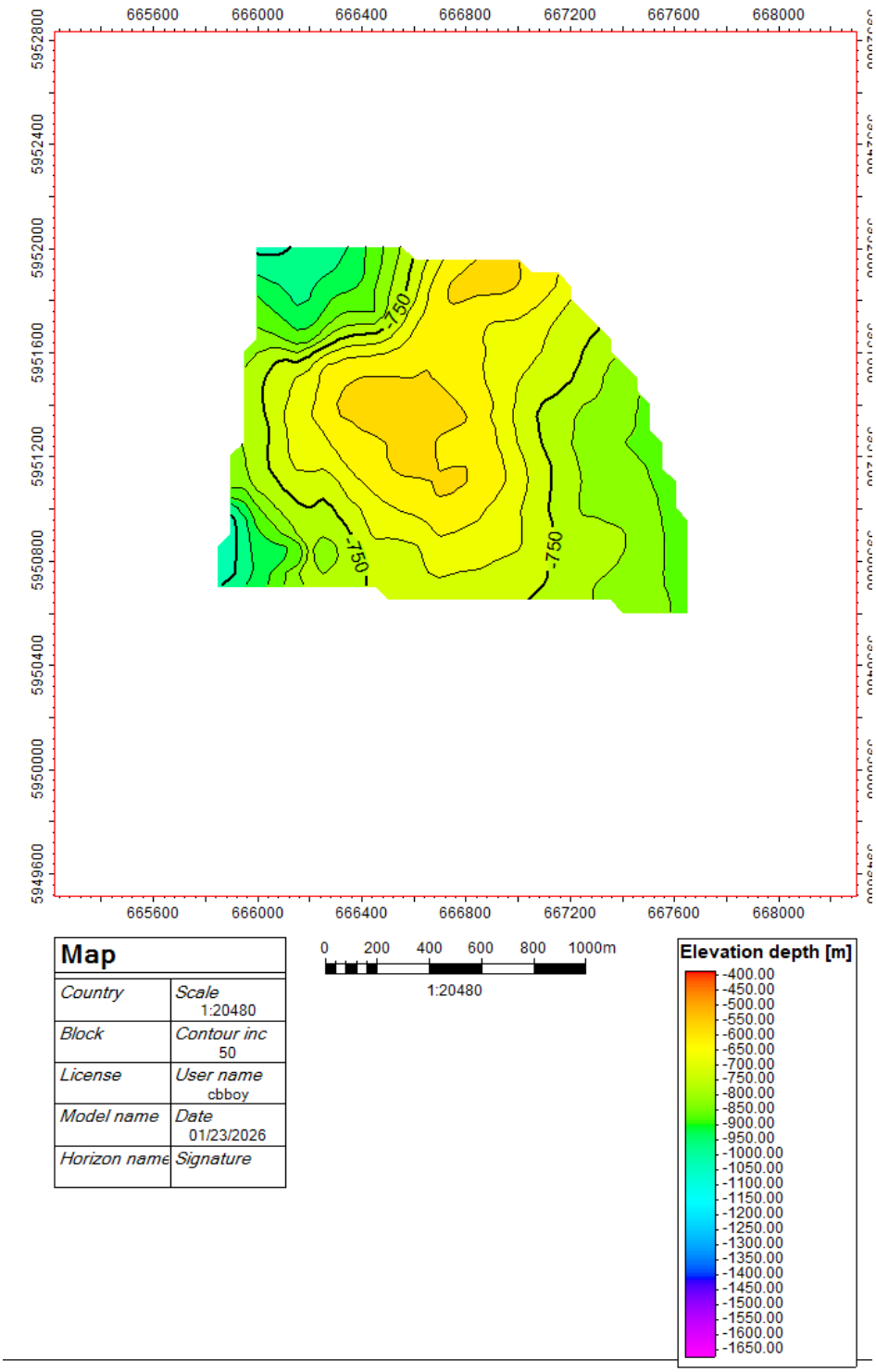

M08 NL base surface

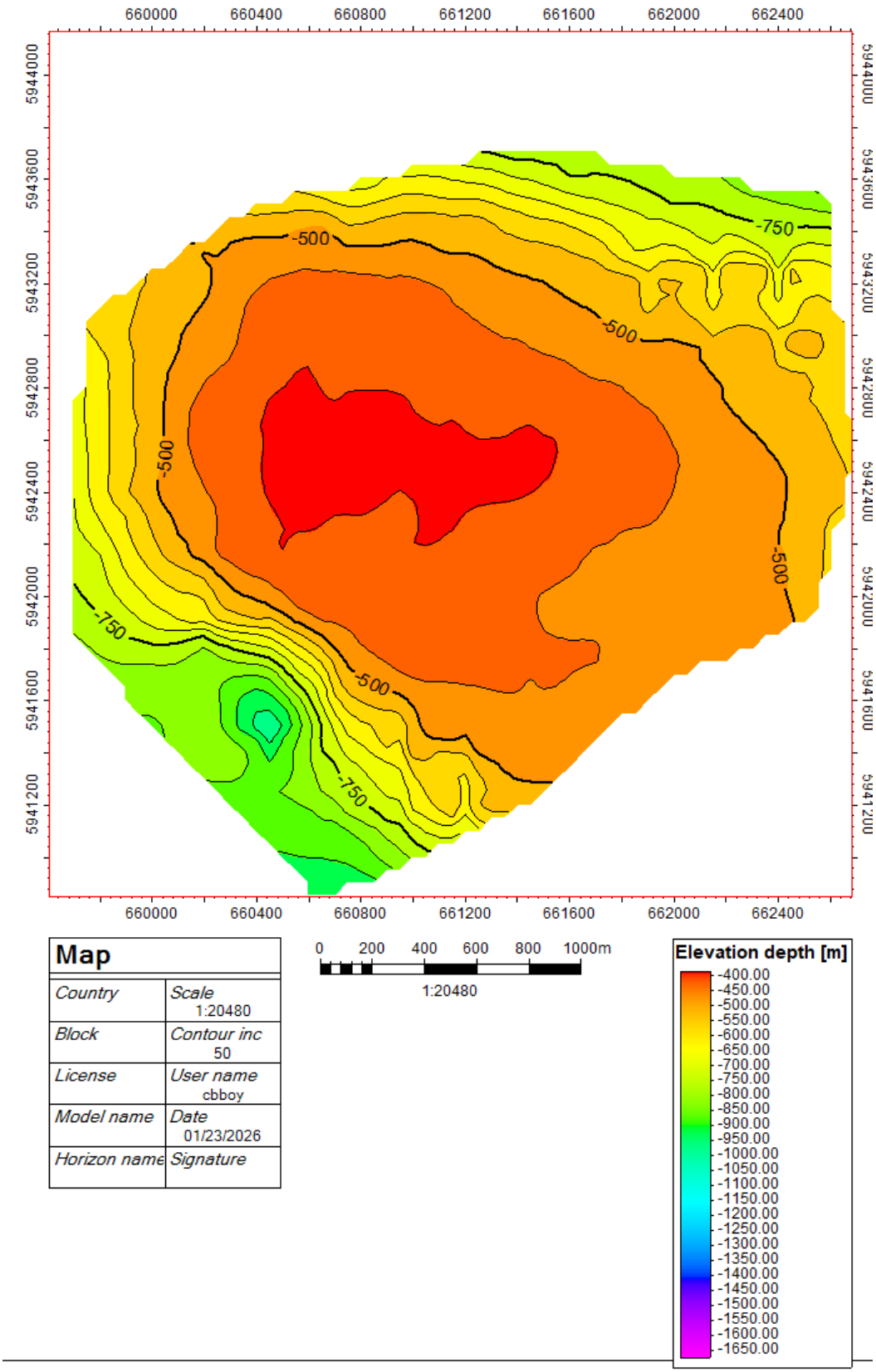

M05-1 NL base surface

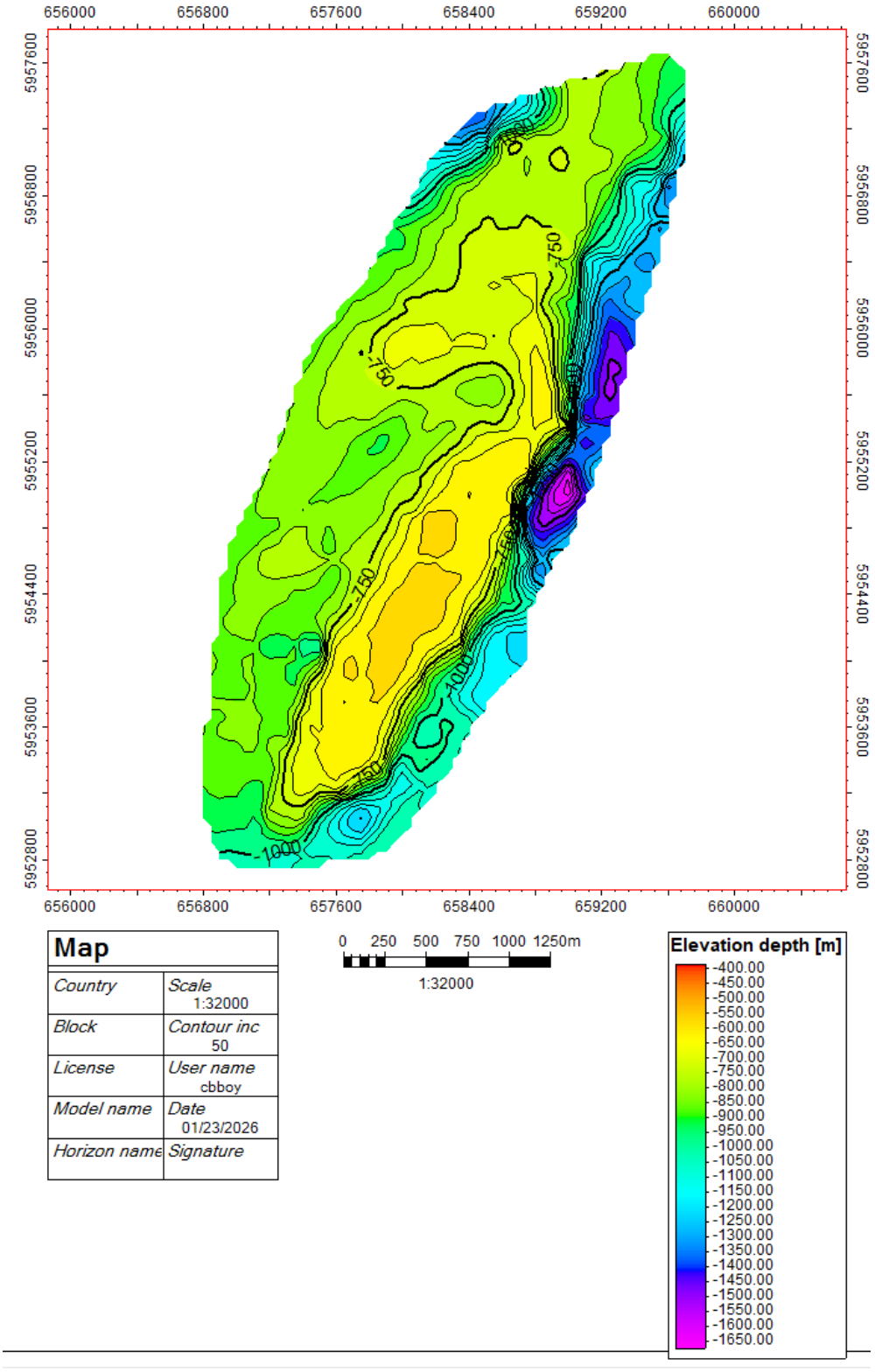

M05-1 NU base surface

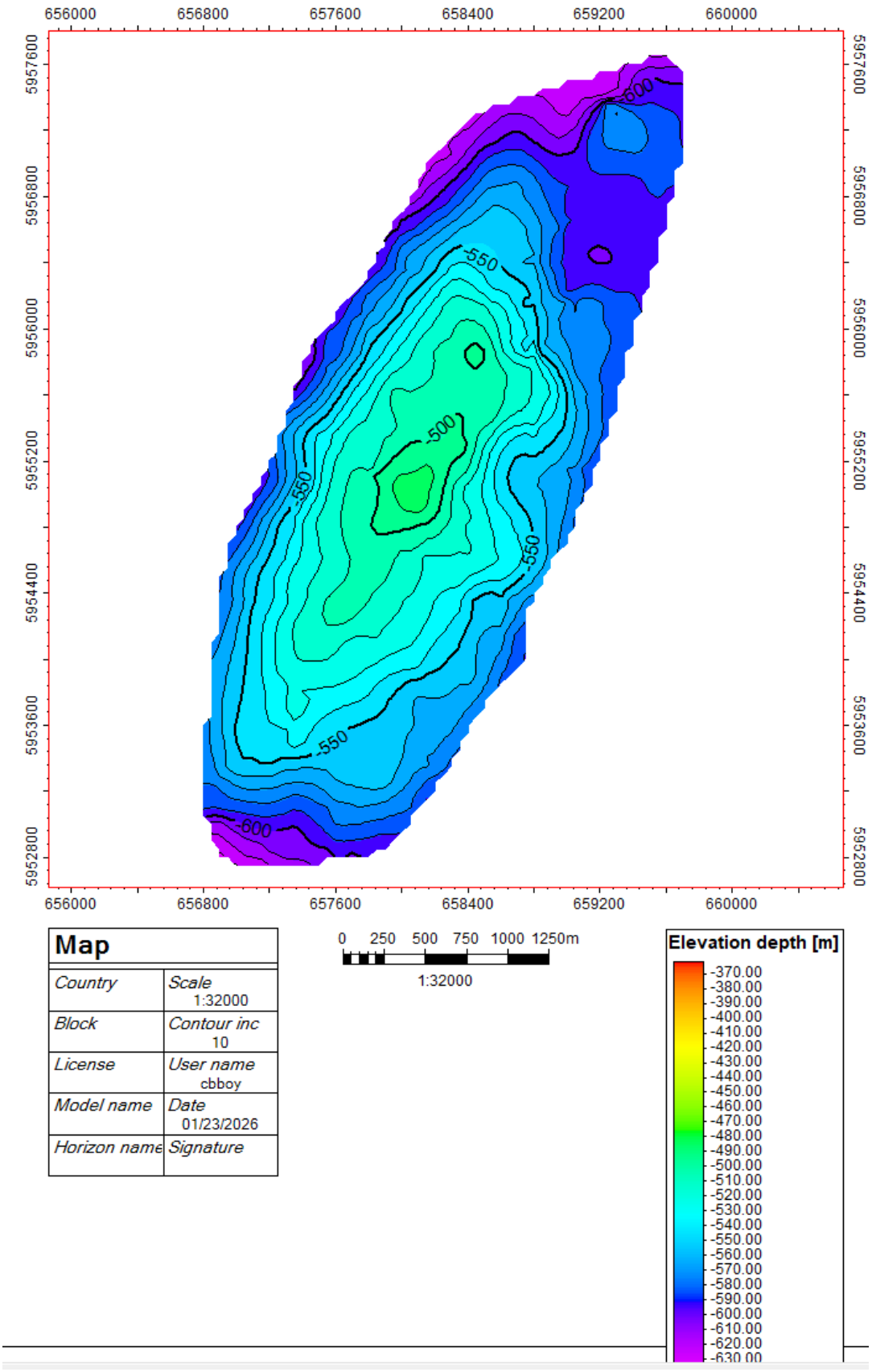

M05-2 NU base surface

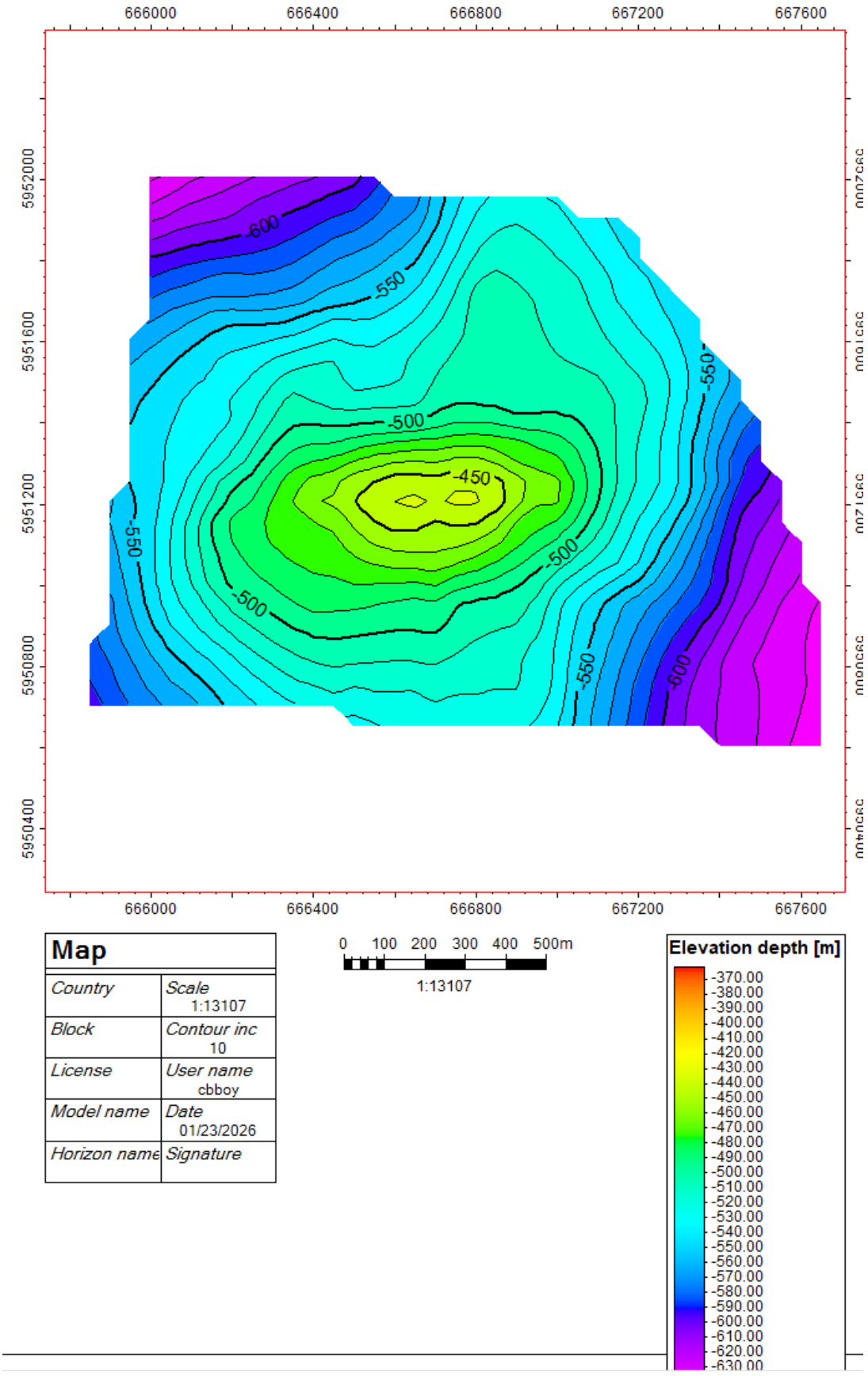

M08 NU base surface

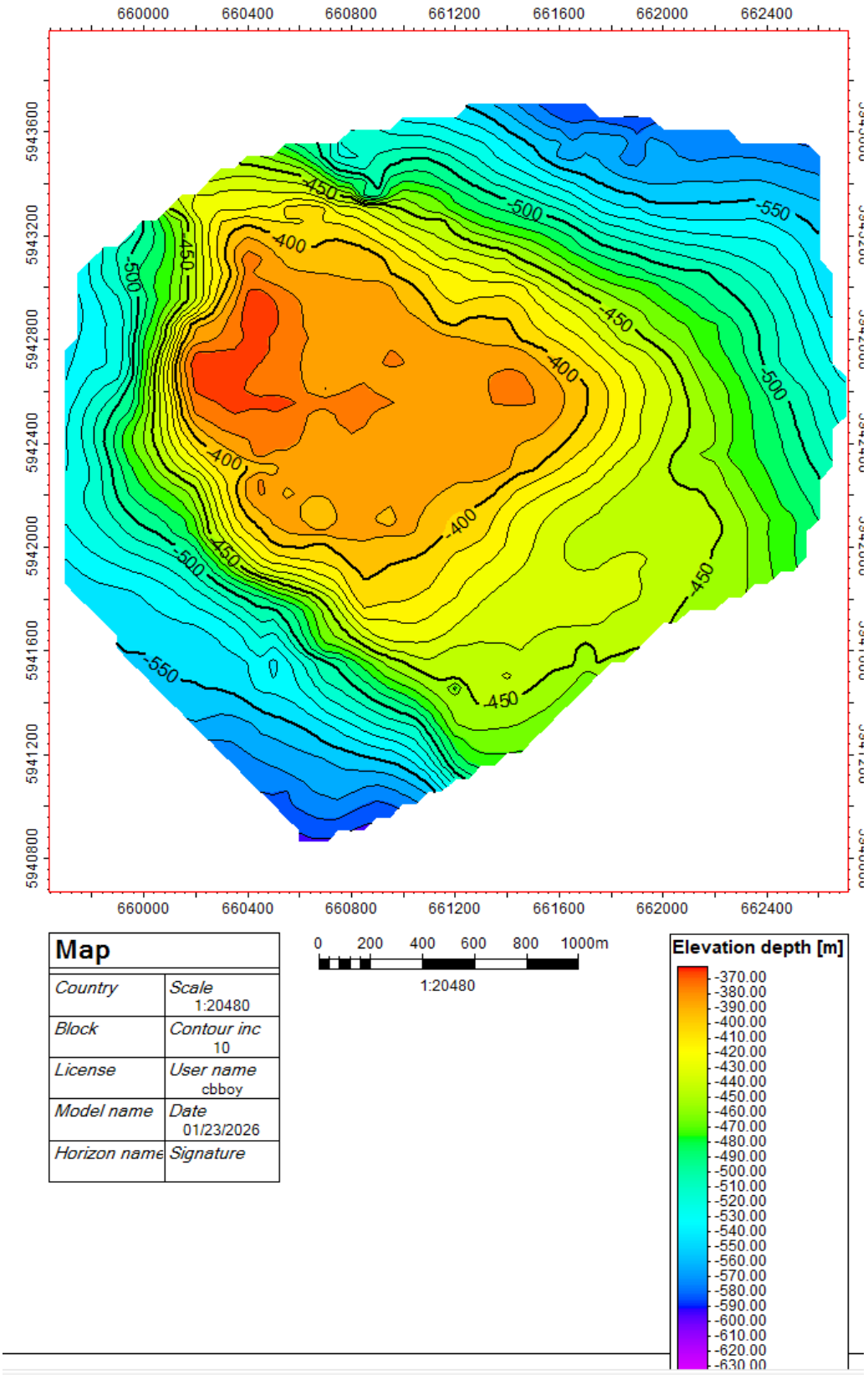

Layout of lower (400m x 650m) and higher (400m x 770m) level repository inside the Pieterburen salt diapir.

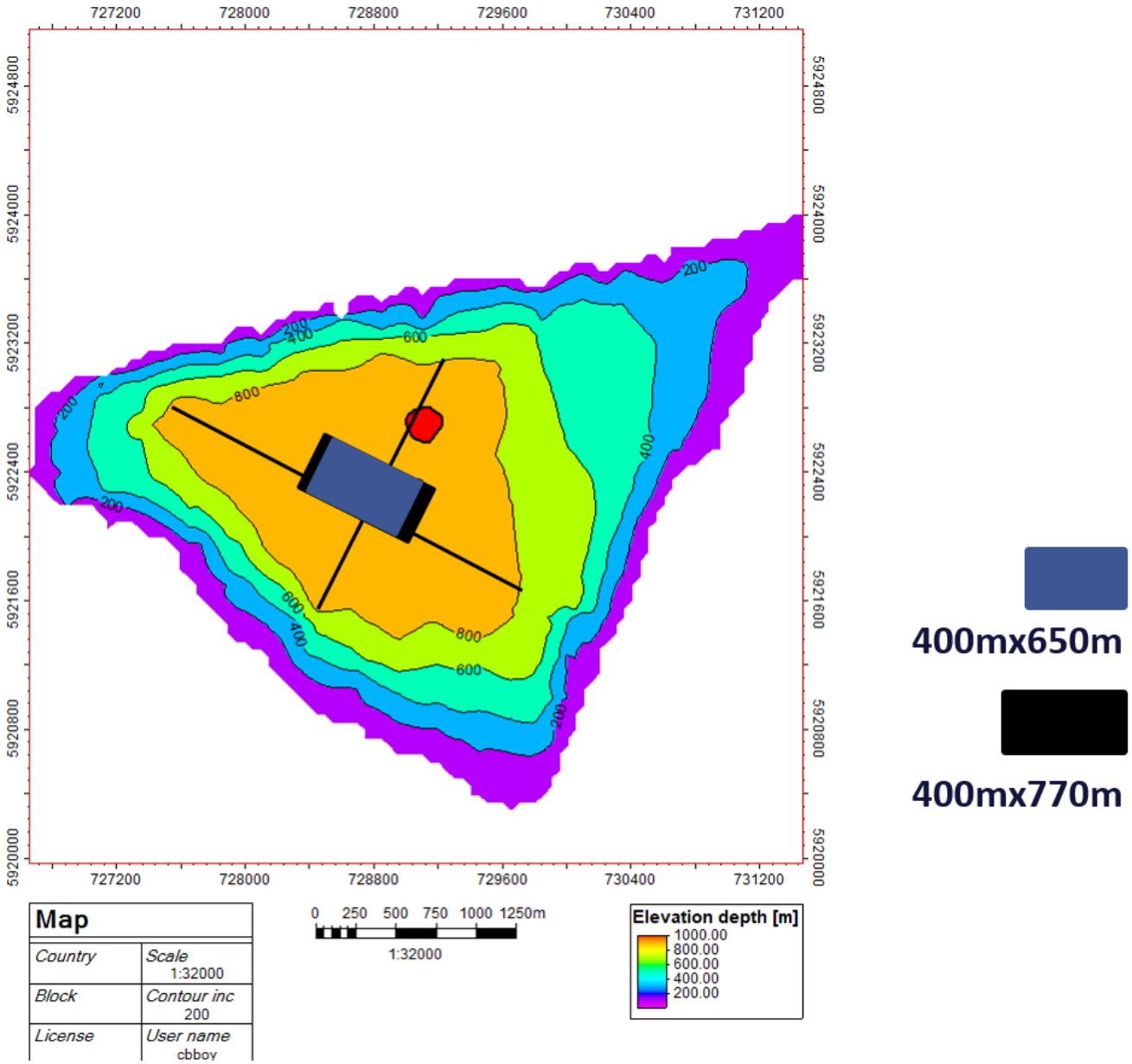

Layout of lower (400m x 650m) and higher (400m x 770m) level repository inside the M08 salt diapir.

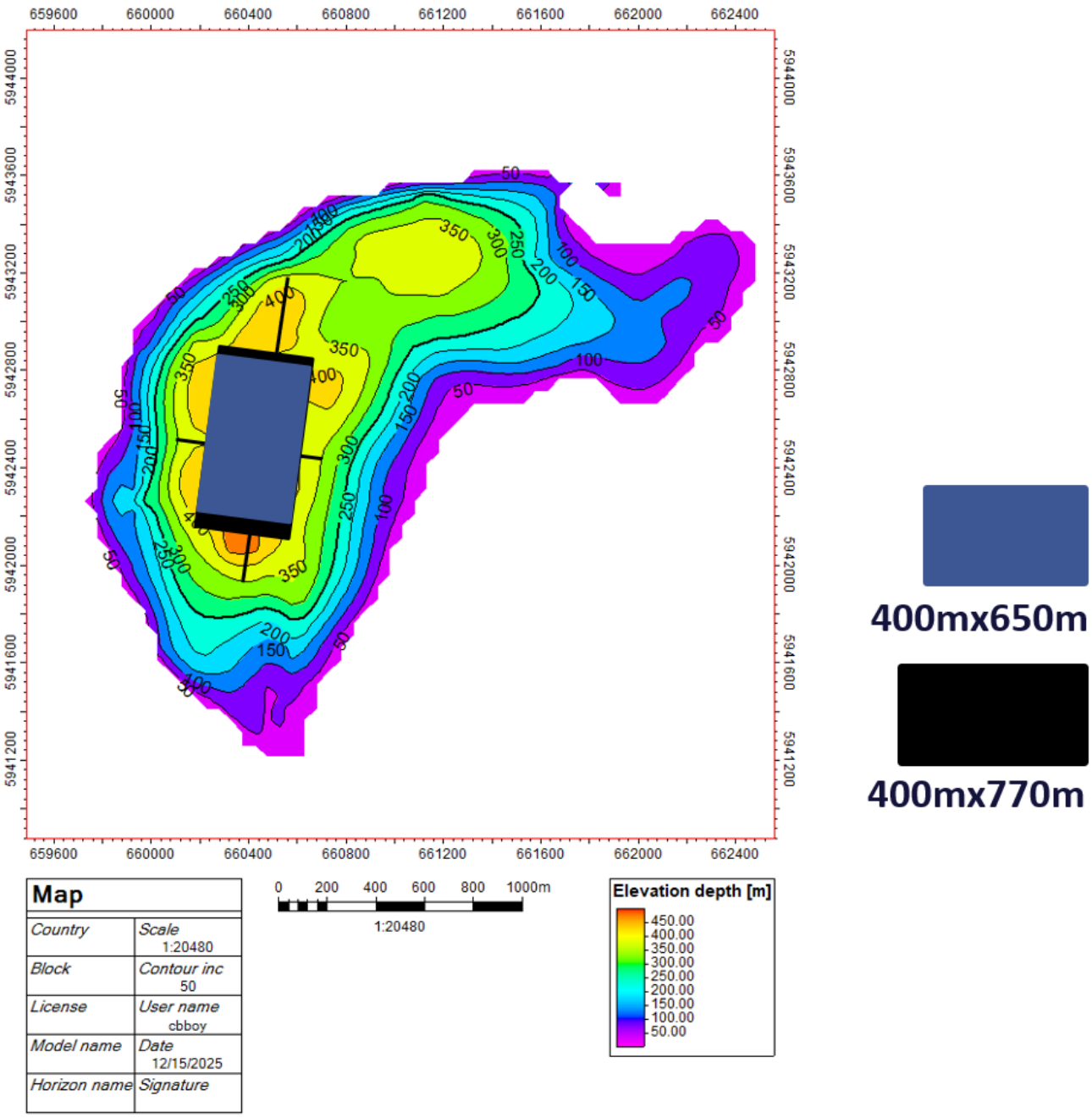

Layout of lower (400m x 650m) and higher (400m x 770m) level repository inside the M05-2 salt diapir.

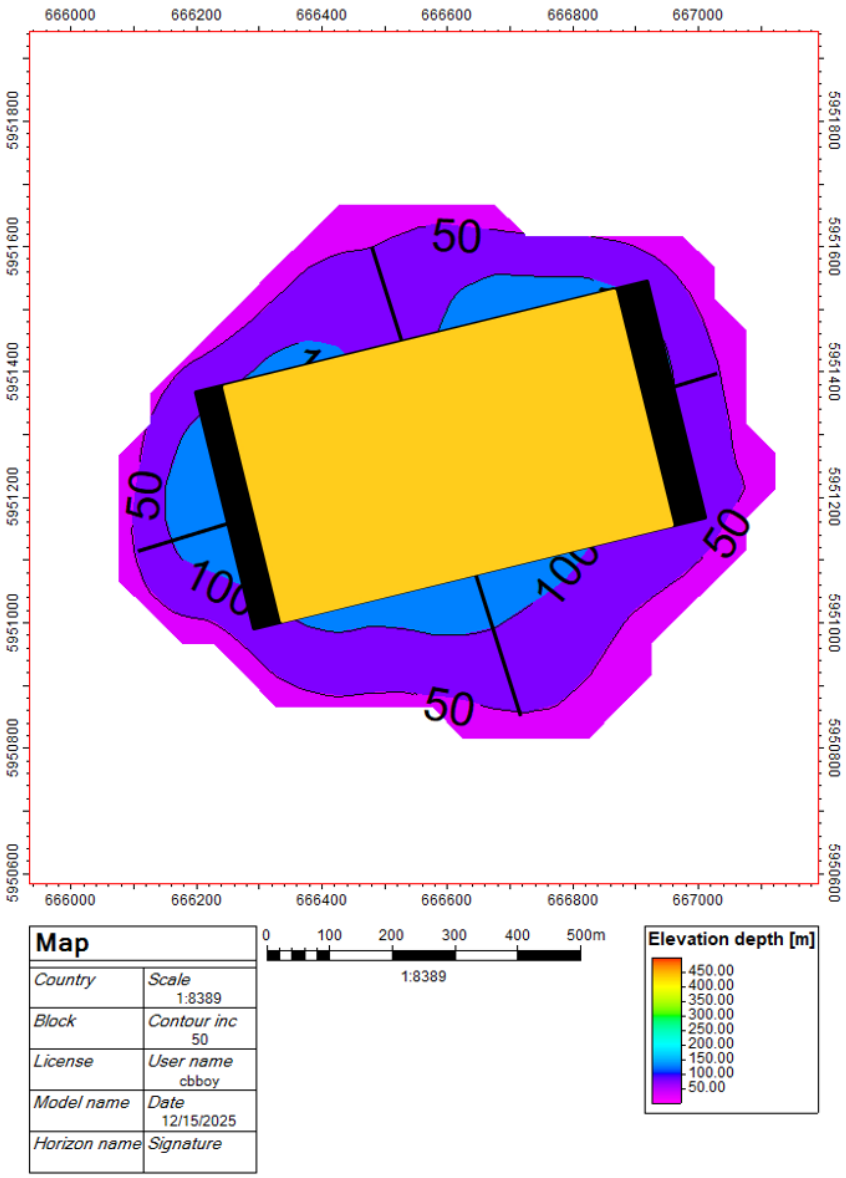

400mx650m

400mx770m